KRYLOV BOGOLIUBOV TYPE ANALYSIS OF VARIANTS OF THE MATHIEU EQUATION

B Shayak[(1), (3)]

Pranav Vyas[(2)]

[(1)]Department of Physics, [(2)]Department of Mechanical Engineering
Indian Institute of Technology Kanpur
NH-91, Kalyanpur
Kanpur – 208016
Uttar Pradesh, INDIA

[(3)]Current affiliation :
Department of Theoretical and Applied Mechanics and Mechanical Engineering
Cornell University
Ithaca, New York – 14853
USA

email : Shayak – shayak@iitk.ac.in, shayak12424@yahoo.in, sb2344@cornell.edu Pranav – vpranav@iitk.ac.in

*

Classification

PACS : 05.45.-a 85.70.-w 02.60.-x

Keywords : Quasiperiodic parametric excitation and drive Extended Krylov-Bogoliubov technique

Abstract

In this work we show that a Krylov-Bogoliubov type analysis is a powerful method for analysing variants of the Mathieu equation. We first demonstrate the technique by rederiving the results obtained by prior authors using different techniques and then apply it to a case where the system has a quasiperiodic drive (inhomogeneity) in addition to a quasiperiodic parametric term. A realistic system where such a forcing is present is an induction motor, so we adopt that as our model system to show the details of the method.

* * * * *

Introduction

The Mathieu equation for dynamical systems (and its variant, the Bloch equation of quantum mechanics) have been around for about a century [1], but it is only recently, with the advent of modern computational technology, that a comprehensive analysis of extensions and variations on the basic equation has been performed. One of the primary workers in the field is RICHARD RAND; he and his collaborators have performed extensive research into quasiperiodic Mathieu equations [2-5] and equations with nonlinearity and damping [3,6]. An extension to two-dimensional systems has been done by THOMAS WATERS [7]. GERTRUD KOTOWSKI [8] has considered a Mathieu equation with external forcing (inhomogeneity) while MOHAMED BELHAQ and his co-workers [9,10] have considered the case where inhomogeneity is added to a nonlinear Mathieu equation. This produces a quasiperiodic response from the system. The primary analytical technique used by these authors is the method of multiple scales (slow and fast) – RAND and his coauthors have also performed harmonic balance.

In this paper we show that a common technique to derive all the previous results is the averaging invented by NIKOLAI MITROFANOVICH KRYLOV and NIKOLAI NIKOLAYEVICH BOGOLIUBOV; this is also applicable to more complicated situations where the other methods can be difficult in practice. In Section 1 we introduce the method and use it to rederive some of the past work. We then present the class of problem which is the primary focus of this paper – namely a system featuring quasiperiodic forcing as both parametric excitation and external drive. In Section 2 we consider a physically realistic system where such a situation occurs – this is the induction motor with a quasiperiodic stator current. In Section 3 we obtain the nature of the solution trajectories and then perform the stability analysis in Section 4. Thus, the first Section serves to demonstrate the effectiveness of the proposed method in standard cases, whereas the subsequent Sections apply it to a novel and more difficult case.

1. Basics of the Krylov-Bogoliubov method

The Krylov-Bogoliubov method is as follows : given a complicated differential equation we assume a solution which is periodic or is the sum of finitely many periodic terms. The constituent frequencies are obtained from inspection. We then tack on time-varying amplitudes to each frequency component, substitute the modified ansatz into the original equation and simplify the resultant equations assuming that the amplitude modulation of each wave component is slow. The amplitude dynamics conveys information about the stability of the solutions being sought. Despite sounding simple in theory, the method is quite difficult to apply in practice and so is often not a first line approach for analysis of an arbitrary nonlinear or otherwise unsolvable system.

In this Section we present a brief survey of the methods already used in the literature, and demonstrate how Krylov-Bogoliubov method can be used to obtain all the results presented in prior works. We first consider the resonance structure in the quasiperiodic Mathieu equation, which has been discussed by RAND and his coauthors. In the first paper [2], the equation considered by the authors is

$$\ddot{x} + \left[\delta + \varepsilon\left(\cos t + \cos \omega t\right)\right] x = 0 \quad , \tag{1}$$

and their work focuses on the instability tongues originating from a resonance between the natural frequency and the driving frequencies. Specifically, they use a perturbative ansatz

$$\delta = \Omega^2 + \delta_1 \varepsilon + \delta_2 \varepsilon^2 + ... \quad , \tag{2a}$$

and examine the case where $\Omega = \left(n + m\omega\right)/2$. At the boundaries of the stability tongues, the motions are periodic, as obtained from a harmonic balance analysis. Further, the authors have used a singular perturbation method based on separation of slow and fast time scales near the point ω=0. Their final results are in Eqs. (23) and (25), which are the slow flow evolution equations. A closely related work is [5] where a 2:2:1 resonance has been analysed using the scale separation method. An extension to the case of nonlinear Mathieu equation has been done in Reference [6] which has a viscous damping term and a Duffing type nonlinear term. Once again, the authors work near the 2:2:1 resonance and use a scale separation approach to obtain their primary equations, Eqs. (21) and (22).

A common platform is a synthesis of the different approaches into a unified Krylov-Bogoliubov approach. For the case of [2], where ω=Δ is $O(\varepsilon)$ we can use the ansatz

$$x(t) = A(t)\cos\left(\frac{t}{2} + \theta\right) \quad , \tag{3}$$

where A and θ are slowly varying functions of time. This implies that $\ddot{A} << \dot{A}$, $\ddot{\theta} << \dot{\theta}$ and second order terms like $\dot{A}\dot{\theta}$, $\dot{A}^2$ and $\dot{\theta}^2$ are negligible. Using an expansion $\delta = \frac{1}{4} + \delta_1\varepsilon + \delta_2\varepsilon^2 + ...$, substituting all this into (1) and equating the coefficients of cosine and sine terms gives

$$\dot{A} = \frac{\varepsilon}{2}\sin 2\theta \quad , \tag{4a}$$

$$\dot{\theta} = \varepsilon\delta_1 A + \frac{\varepsilon}{2}\cos 2\theta + \varepsilon\cos\Delta\varepsilon t \quad . \tag{4b}$$

Defining slow time $\tau = \varepsilon t$ and $\Delta' = \varepsilon\Delta$ we get

$$\frac{\mathrm{d}A}{\mathrm{d}\tau} = \frac{1}{2}\sin 2\theta \quad , \tag{5a}$$

$$\frac{\mathrm{d}\theta}{\mathrm{d}\tau} = \delta_1 A + \frac{1}{2}\cos 2\theta + \cos\Delta'\tau \quad , \tag{5b}$$

which are in exact agreement with Eqs. (23) and (25) of [2].

An identical ansatz reproduces the result of RAND et. al. [5], where they have worked near the 2:2:1 resonance. Following the Krylov-Bogoliubov ansatz we obtain the amplitude equations

$$\dot{A} = -\frac{\varepsilon A}{2}\sin 2\varphi - \frac{\varepsilon\mu A}{2}\sin\left(2\varphi - \varepsilon\Delta t\right) \quad , \tag{6a}$$

$$\dot{\varphi} = -\delta_1\varepsilon - \frac{\varepsilon}{2}\cos 2\varphi - \frac{\varepsilon\mu A}{2}\cos\left(2\varphi - \varepsilon\Delta t\right) \quad . \tag{6b}$$

Once again rescaling the time and the frequency, we have

$$\frac{\mathrm{d}A}{\mathrm{d}\tau} = -\frac{A}{2}\sin 2\varphi - \frac{\mu A}{2}\sin\left(2\varphi - \Delta'\tau\right) \quad , \tag{7a}$$

$$\frac{\mathrm{d}\varphi}{\mathrm{d}\tau} = -\delta_1 - \frac{1}{2}\cos 2\varphi - \frac{\varepsilon\mu}{2}\cos\left(2\varphi - \Delta\tau\right) \quad , \tag{7b}$$

which are in agreement with Eqs. (8) and (9) of Ref. [5].

Finally, we use the approach to derive the results in the third work by RAND et. al. [6] where the same ansatz gives

$$\dot{A} = -\frac{\mu\varepsilon c}{2}A - \frac{\varepsilon A}{2}\sin 2\varphi - \frac{\varepsilon\mu A}{2}\sin\left(2\varphi - \Delta\varepsilon t\right) - \mu\varepsilon cA\dot{\varphi} \quad , \tag{8a}$$

$$A\dot{\varphi} = -\varepsilon\delta_1 A - \frac{\varepsilon A}{2}\cos 2\varphi - \frac{\varepsilon\mu A}{2}\cos\left(2\varphi - \varepsilon\Delta t\right) - \frac{3}{4}\lambda A^3 - \mu\varepsilon c\dot{A} \quad . \tag{8b}$$

Now since $\dot{A}$ and $\dot{\varphi}$ are both $O(\varepsilon)$, the last terms on the right hand side (RHS) of both the above equations can be dropped. Then rescaling the time gives

$$\frac{\mathrm{d}A}{\mathrm{d}\tau} = -\frac{\mu c}{2}A - \frac{1}{2}A\sin 2\varphi - \frac{\mu}{2}A\sin\left(2\varphi - \Delta\tau\right) \quad , \tag{9a}$$

$$\frac{\mathrm{d}\varphi}{\mathrm{d}t} = -\delta_1 - \frac{\varepsilon}{2}\cos 2\varphi - \frac{\mu}{2}\cos\left(2\varphi - \Delta\tau\right) - \frac{3}{4}\lambda A^2 \quad . \tag{9b}$$

To compare this result with Ref. [6] we first change variable from A to R in (9). We then take their Eqs. (11) and (12), write $A = R\cos\varphi$ and $B = -R\sin\varphi$, obtain the time derivatives of these quantities and see that the results are identical to what we have found above.

A different kind of system has been considered by BELHAQ and M HOUSSNI [9] :

$$\ddot{x} + \alpha\dot{x} + \omega_0^2 x + h\cos\left(\nu t\right)x + \beta x^2 + \xi x^3 = \gamma\cos\omega t \quad , \tag{10}$$

i.e. a Mathieu equation with an external forcing (inhomogeneous) term. They carry out their analysis near resonances, i.e. when

$$\omega_0^2 = \left(\frac{p}{q}\omega\right)^2 + \delta \quad , \tag{11}$$

in which p and q are natural numbers and δ is a small detuning parameter. If $h=0$ then $p/q=1$ gives the primary resonance; higher order resonances can be found when $\beta=0$ and $p/q=1/3$ and when $\xi=0$ and $p/q=1/2$ (resonances corresponding to the cubic and quadratic nonlinearities respectively). To analyse the primary resonance using the Krylov-Bogoliubov formalism we write $x = A(t)\cos\left[\omega t + \varphi(t)\right]$ and then substitute this into (11) to get

$$\dot{A} = -kA - \frac{\gamma}{2\omega}\sin\varphi \quad , \tag{12a}$$

$$\dot{\varphi} = \frac{\delta}{2\omega} - \frac{\gamma}{2\omega A}\cos\varphi + \frac{3\lambda}{8\omega}A^2 \quad . \tag{12b}$$

This can be compared with Eq. (6) of the Reference, after its fast variation on account of the $\dot{\theta}$ term is averaged out. Similarly, expressions for the other resonances can also be derived but let us now switch from derivation of past work to presentation of our own original contributions.

One of the features of the works cited above is that they are interested primarily in the periodic solutions which occur near the resonances. An important question to investigate is what happens if a quasiperiodic forcing term is introduced into a quasiperiodic Mathieu equation. That is, we consider an equation of the form

$$\ddot{x} + \omega^2 x + 2\varepsilon\left(\cos t + \cos\Omega t\right)x = F\left(\cos t + \cos\Omega t\right) \quad . \tag{13}$$

To gain some insight into the system we first simulate it using the value Ω=0.707, 2ε=0.1 and F=1. For a 'typical' ω value of 2.5, a bounded quasiperiodic response is observed. When ω is set equal to 1, however, an ordinary resonance is seen – the motion is nearly periodic and its amplitude is linearly increasing with time. A similar resonance is seen when ω=0.707, the other driving frequency. A strong parametric resonance is observed when ω=0.5 or 0.3535 (half of either driving frequency) – this is similar to the 2:2:1 resonance observed by RAND et. al. These three cases are shown in the three panels of Fig. 2.

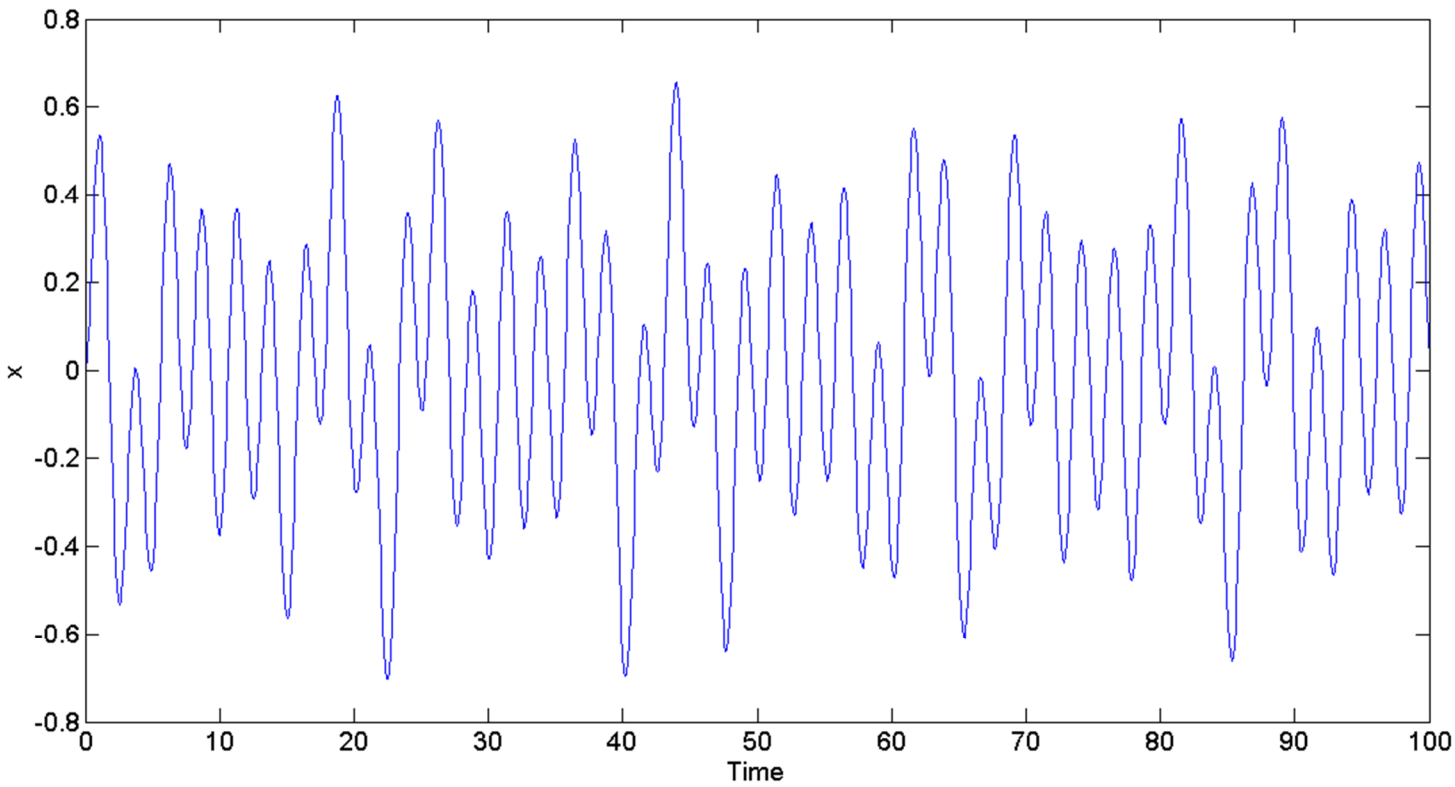

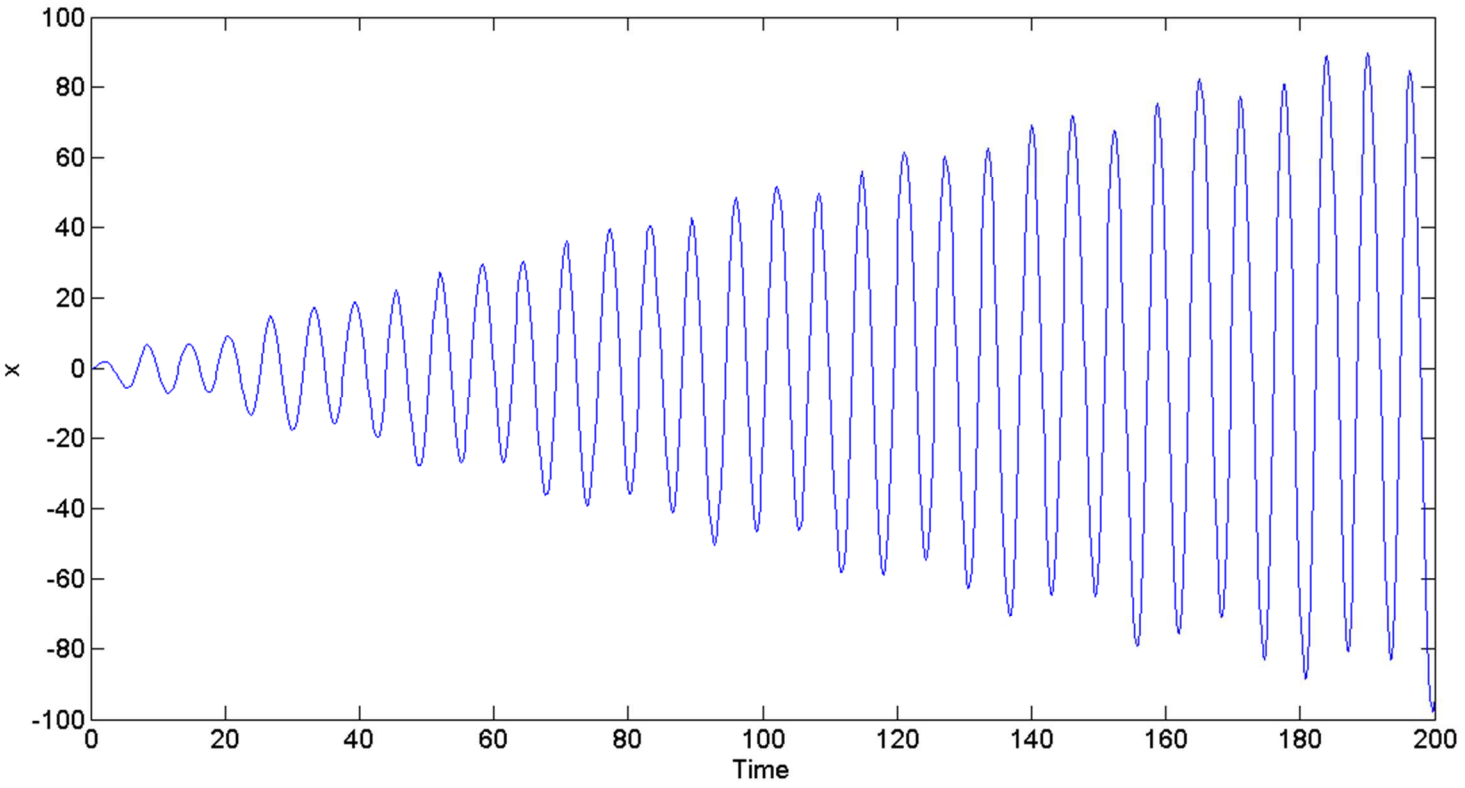

Figure 1 : *Upper panel shows ω=2.5 – the quasiperiodic motion is quite evident. In the middle panel, ω=1 and there is a resonance. Note that the amplitude growth here is linear : the amplitude is significant very early on into the motion and then keeps increasing slowly and steadily. The lowest panel has ω=0.49 and there is a subharmonic parametric resonance. Note that the amplitude growth here is exponential : the amplitude is negligible for a long time and then it explodes.*

To analyse the system our Krylov-Bogoliubov ansatz must be of the type

$$x = A_1 \cos t + B_1 \sin t + A_2 \cos \Omega t + B_2 \sin \Omega t + \ldots\ldots \quad , \tag{14}$$

where all the A's and B's are time varying. The form of (13) implies that combination frequencies 1+Ω, 1-Ω and higher harmonics will be generated and must also be included in the above expansion. We do a demonstration here with the fundamental and most basic combination harmonics. We use the expansion

$$x = A_1\cos t + B_1\sin t + A_2\cos\Omega t + B_2\sin\Omega t + A_3\cos(1+\Omega)t + B_3\sin(1+\Omega)t + A_4\cos(1-\Omega)t + B_4\sin(1-\Omega)t \quad , \tag{15}$$

substitute this into (13) and equate separately the cosinusoidal and sinusoidal components at each frequency. This leads to eight equations which are as follows :

$$\ddot{A}_1 + (\omega^2 - 1)A_1 + 2\dot{B}_1 + \varepsilon(A_3 + A_4) - F = 0 \quad , \tag{16a}$$

$$\ddot{B}_1 + (\omega^2 - 1)B_1 - 2\dot{A}_1 + \varepsilon(B_3 + B_4) = 0 \quad , \tag{16b}$$

$$\ddot{A}_2 + (\omega^2 - \Omega^2)A_2 + 2\Omega\dot{B}_2 + \varepsilon(A_3 + A_4) - F = 0 \quad , \tag{16c}$$

$$\ddot{B}_2 + (\omega^2 - \Omega^2)B_2 - 2\Omega\dot{A}_2 + \varepsilon(B_3 - B_4) = 0 \quad , \tag{16d}$$

$$\ddot{A}_3 + \left[\omega^2 - (1+\Omega)^2\right]A_3 + 2(1+\Omega)B_3 + \varepsilon(A_1 + A_2) = 0 \quad , \tag{16e}$$

$$\ddot{B}_3 + \left[\omega^2 - (1+\Omega)^2\right]B_3 - 2(1+\Omega)A_3 + \varepsilon(B_1 + B_2) = 0 \quad , \tag{16f}$$

$$\ddot{A}_4 + \left[\omega^2 - (1-\Omega)^2\right]A_4 + 2(1-\Omega)B_4 + \varepsilon(A_1 + A_2) = 0 \quad , \tag{16g}$$

$$\ddot{B}_4 + \left[\omega^2 - (1-\Omega)^2\right]B_4 - 2(1-\Omega)\dot{A}_4 + \varepsilon(B_1 - B_2) = 0 \quad . \tag{16h}$$

This is an autonomous system whose fixed points and stability features can all be obtained analytically (perhaps facilitated by computer algebra [11]) or numerically. The primary resonances are visible upon inspection alone and the parametric ones will arise if we also include terms featuring cos2t, sin2t etc., as for the ordinary Mathieu equation. A more accurate analysis can be done by considering additional harmonics.

A more fundamental issue which needs to be taken care of is that the system (13) appears contrived, unlike the model systems chosen by the prior authors. The first paper by RAND's group describes an ideal small-oscillations pendulum whose base is excited quasiperiodically and the second paper amplifies on the same system. The third paper adds viscous damping and cubic nonlinearity – not so small oscillations of a realistic pendulum. The first paper by BELHAQ's group [9] describes the above pendulum whose bob is also excited externally. In a subsequent paper by their group [10], the system is a tower and the external excitation is a wind and it has no connection with the parametric excitation which is due to ground forces. But the same quasiperiodic excitation at both the base and the bob of the pendulum in (13) seems like a miraculous coincidence, in other words a physically implausible system.

A device which naturally yields a structure like (13) is an induction motor driven by a quasiperiodic stator current. Its equation of motion is third order and nonlinear and features the same quasiperiodic excitation as both a parametric and an inhomogeneous term. Unlike (13), this is a physical system and we will focus on this system for the remainder of this Article.

2. Equation of motion and basic cases

An induction motor typically consists of two concentric cylinders – the stator, which remains static and the rotor, which rotates. It is shown in the schematic diagram Fig. 2. The stator is generally wound with three phase windings and an inverter is used to supply voltage or current through these windings. These voltages/currents are predetermined functions of time and the inverter is called voltage source and current source accordingly as the quantity which it supplies. The rotor is in the shape of a metal cage and we expect that the current carried in it will be a periodic function of the azimuthal angle θ. At the most basic level, we expect that there will be two components of rotor current, one proportional to cosθ and the other proportional to sinθ. These components are clubbed to form a complex number or phasor (also called vector), thus the rotor current vector $\mathbf{i}_r = i_{r,cos} + \mathrm{j}\, i_{r,sin}$ where j denotes the imaginary unit. The real and imaginary parts of a phasor are of course the respective cos and sin components. An elegant formulation of the dynamic equation, first proposed by KOVACS and RACZ [12], is achieved in terms of these phasors. Here we motivate the equation structure obtained by them. Using Lenz's law we can write the rotor voltage as the rate of change of flux. The flux in turn is $L_r\mathbf{i}_r + M\mathbf{i}_s$ where L_r is the rotor self-inductance, M the mutual inductance and $\mathbf{i}_s$ the stator current. Now the time derivative will not be simple because of the rotation of the rotor; the differential operator in fact acquires the structure $\mathrm{d}/\mathrm{d}t - \mathrm{j}\omega$. Finally, we apply Kirchhoff's law to get (17a) below. The torque on the rotor is generated by interaction between the rotor current and the stator magnetic field : careful bookkeeping of the signs etc. leads to the expression in the last term of (17b), which expresses Newton's law for the motor.

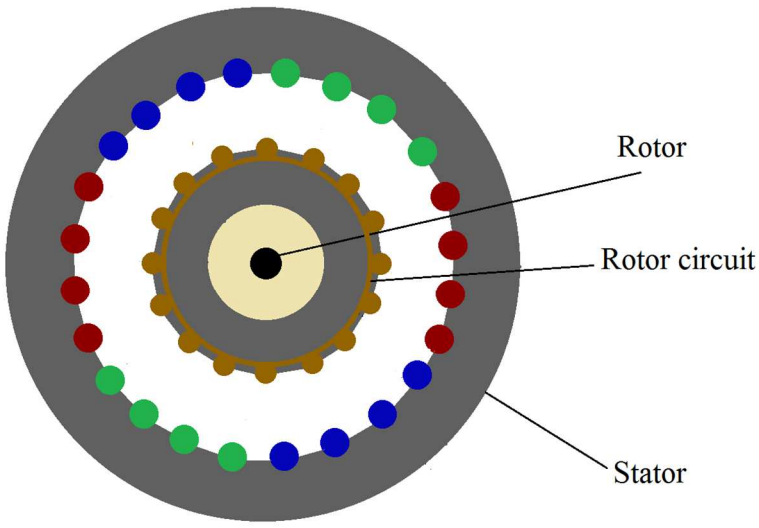

Figure 2 : *A schematic diagram of the induction motor. The rotor is shaped like a squirrel cage. The stator is designed so that it creates a rotating magnetic field.*

We write the equation in non-dimensionalized form, using $\tau = L_r / R_r$ and $\delta = M / L_r$. Hence, τ denotes the rotor time constant while δ is a dimensionless number less than unity. Further, we denote the moment of inertia of the rotor and load by J and the drag torque on the motor by Γ and write Newton's law to get the equation of motion

$$\frac{\mathrm{d}}{\mathrm{d}t}\mathbf{i}_r + \left(\frac{1}{\tau} - \mathrm{j}\omega\right)\mathbf{i}_r = -\delta\left(\frac{\mathrm{d}}{\mathrm{d}t} - \mathrm{j}\omega\right)\mathbf{i}_s \quad , \tag{17a}$$

$$J\frac{\mathrm{d}}{\mathrm{d}t}\omega = T - \Gamma = C\mathbf{i}_r \cdot \left(-\mathrm{j}\mathbf{i}_s\right) - \Gamma \quad , \tag{17b}$$

in which C is a positive constant determined by rotor geometry and for two phasors $\mathbf{X}$ and $\mathbf{Y}$, $\mathbf{X}\cdot\mathbf{Y} = \mathrm{Re}(X)\mathrm{Re}(Y) + \mathrm{Im}(X)\mathrm{Im}(Y)$.

We would like to emphasize that the concepts involved in the derivation of (17) play no further role in this Article, hence readers unfamiliar with induction motors can safely start from this point, visualizing $\mathbf{i}_r$ and ω as generalized dynamical variables and treating (17) as a given equation of motion.

We now consider the case where $\mathbf{i}_s$ is a quasiperiodic function of time i.e. $\mathbf{i}_s = i_1 \exp \mathrm{j}\left(\Omega_1 t\right) + i_2 \exp \mathrm{j}\left(\Omega_2 t\right)$ where Ω_1 and Ω_2 are incommensurate. Further we take δ to be equal to unity for simplification and obtain the following equation :

$$\frac{\mathrm{d}}{\mathrm{d}t}\mathbf{i}_r + \left(\frac{1}{\tau} - \mathrm{j}\omega\right)\mathbf{i}_r = \left(-\Omega_1 + \omega\right) i_1 \exp \mathrm{j}\left(\Omega_1 t\right) + \left(-\Omega_2 + \omega\right) i_2 \exp \mathrm{j}\left(\Omega_2 t\right) \quad , \tag{18a}$$

$$J\frac{\mathrm{d}\omega}{\mathrm{d}t} = C_0 \mathbf{i}_r \cdot \left[-\mathrm{j} i_1 \exp \mathrm{j}\left(\Omega_1 t\right) - \mathrm{j} i_2 \exp \mathrm{j}\left(\Omega_2 t\right)\right] - \Gamma \quad . \tag{18b}$$

Despite the elegance of this representation, the presence of j makes the analysis complex later on, so we also present the system in terms of all real variables $i_{r,cos}$ and $i_{r,sin}$ which for compactness of notation we now write as i_{ra} and i_{rb} :

$$\frac{\mathrm{d}}{\mathrm{d}t} i_{ra} + \frac{1}{\tau} i_{ra} + \omega i_{rb} = i_1\left(\Omega_1 - \omega\right)\sin\Omega_1 t + i_2\left(\Omega_2 - \omega\right)\sin\Omega_2 t \quad , \tag{19a}$$

$$\frac{\mathrm{d}}{\mathrm{d}t} i_{rb} + \frac{1}{\tau} i_{rb} - \omega i_{ra} = -i_1\left(\Omega_1 - \omega\right)\cos\Omega_1 t - i_2\left(\Omega_2 - \omega\right)\cos\Omega_2 t \quad , \tag{19b}$$

$$J\frac{\mathrm{d}}{\mathrm{d}t}\omega = C_0\left[i_{ra}\left(i_1 \sin\Omega_1 t + i_2 \sin\Omega_2 t\right) - i_{rb}\left(i_1 \cos\Omega_1 t + i_2 \cos\Omega_2 t\right)\right] - \Gamma \quad . \tag{19c}$$

Note that (18) and (19) are entirely equivalent so far as actual physical and mathematical content are concerned. This system has the following salient features :

- It is third order when expressed in real variables.
- There is a nonlinear coupling between ω and $\mathbf{i}_r$.
- The term $\omega\left(i_1 \mathrm{e}^{\mathrm{j}\Omega_1 t} + i_2 \mathrm{e}^{\mathrm{j}\Omega_2 t}\right)$ and similar terms in (18b) introduce a quasiperiodic parametric excitation.s

- There are also driving (inhomogeneous) terms which are quasiperiodic with the same frequencies as the parametric excitation.

Thus our system captures the basic features of (13) in a realistic setting. To get a handle on the potential solutions we first make the drastic simplification $\Omega_1=\Omega_2=\Omega$. For this part, the complex representation (18) is the simplest. Inspection yields one possible trajectory of $\mathbf{i}_r$ and ω : the first one assumes the form (...)expj(Ωt), and since both applied and rotor current vectors are rotating at frequency Ω their dot product becomes a constant; if this constant multiplied by C_0 equals the load Γ then ω also becomes constant, and this is consistent with the form of $\mathbf{i}_r$ assumed in (18a). Substituting this ansatz into (18) yields

$$\omega=\omega_0=\text{const.} \quad , \tag{20a}$$

$$\mathbf{i}_r=\frac{-\mathrm{j}\tau(\Omega-\omega_0)(i_1+i_2)}{1+\mathrm{j}\tau(\Omega-\omega_0)}\exp\mathrm{j}(\Omega t) \quad . \tag{20b}$$

Here we omit the process of determination of ω_0 which actually follows by substituting the $\mathbf{i}_r$'s corresponding to different ω_0's into the RHS of (18b) and finding when it becomes equal to zero. What is interesting is the nature of the solution we have obtained; since it is a periodic solution with an amplitude independent of initial conditions (these do not enter (20) in any manner), it must be a limit cycle. The stability of this cycle is proved by a straightforward Krylov-Bogoliubov analysis, this time using the real form (19) of the equation of motion [13]. We do not dwell on the details but merely state that the limit cycle is stable under all circumstances, and the system converges to this cycle from practically any initial condition.

A derivative case is the one where the two frequencies Ω_1 and Ω_2 differ only slightly. Let the average frequency $\Omega_+=(\Omega_1+\Omega_2)/2$ and the differential frequency $\Omega_-=(\Omega_2-\Omega_1)/2$. Then (19) can be written as (using $i_0=i_1+i_2$)

$$\frac{\mathrm{d}}{\mathrm{d}t}i_{rd}+\frac{1}{\tau}i_{rd}+\omega i_{rb}=2i_0(\Omega_+-\omega)\sin\Omega_+t\cos\Omega_-t \quad , \tag{21a}$$

$$\frac{\mathrm{d}}{\mathrm{d}t}i_{rb}+\frac{1}{\tau}i_{rb}-\omega i_{ra}=-2i_0(\Omega_+-\omega)\cos\Omega_+t\cos\Omega_-t \quad , \tag{21b}$$

$$J\frac{\mathrm{d}}{\mathrm{d}t}\omega=2C_0\left[i_{ra}\sin\Omega_+t\cos\Omega_-t-i_{rb}\cos\Omega_+t\cos\Omega_-t\right]-\Gamma \quad . \tag{21c}$$

Now because Ω_1 and Ω_2 are chosen nearly equal, Ω_- is small and a term like $\cos\Omega_- t$ is slow. Using a separation of scales argument, it can be treated like a constant and pulled out from the RHS of (21a) and (21b); the resulting equations are (19a,b) which admit the known solution (20). Thus, the solution of (21a,b) must be the solution function (20b) modulated by a $\cos\Omega_- t$ term. It remains to be checked whether (21c) is consistent with such a solution; indeed, the $\cos\Omega_-$t parts of i_{ra} and i_{rb} multiply with the similar terms in the RHS of (21c) and produce terms which average out to 1/2 over the long period. This 1/2 cancels with the 2 before the C_0; if J is large enough for the speed to remain more or less constant during one period $2\pi/\Omega_-$ then clearly a solution is feasible where the currents are modulated by the differential frequency and the speed is nearly constant, determined as before by the load balancing condition. The solution thus becomes a simple modification of (20) :

$$\omega=\omega_0=\text{const.} \quad , \tag{22a}$$

$$\mathbf{i}_r=\frac{-\mathrm{j}\tau(\Omega-\omega_0)i_0}{1+\mathrm{j}\tau(\Omega-\omega_0)}\exp\mathrm{j}(\Omega_+t)\cos(\Omega_-t) \quad . \tag{22b}$$

With this we conclude our discussion of the system equation and of the easy cases where the driving frequencies are exactly and almost equal. In the next Section we work in the absence of these restrictive assumptions.

3. Characterizing the quasiperiodic trajectory

We now consider the case where Ω_1 and Ω_2 are arbitrary and are related by an irrational ratio. We expect that the limit cycle of the previous Section will generalize to a limiting quasiperiodic trajectory and we wish to find the nature of this trajectory [14].

The current components, instead of oscillating at one frequency, will pick up more frequencies and the angular velocity too will show an oscillatory component. We may write the ansatz

$$i_{ra}=\sum_k a_k\exp\mathrm{j}(\nu_k t)+a_k{}^*\exp\mathrm{j}(-\nu_k t) \quad , \tag{23a}$$

$$i_{rb}=\sum_k b_k\exp\mathrm{j}(\nu_k t)+b_k{}^*\exp\mathrm{j}(-\nu_k t) \quad , \tag{23b}$$

$$\omega = \sum_k c_k \exp \mathrm{j}(\nu_k t) + c_k{}^* \exp \mathrm{j}(-\nu_k t) \quad , \tag{23c}$$

in which ν_k denotes the set of response frequencies exhibited by the system (the index k is being used as i and j are already busy). This set is not known a priori and we will determine it presently. Note that although j appears in (23) and a_k, b_k and c_k are all complex (technically we should have put phasor signs on them but that will only appear confusing), it is the real form (15) of the system equation which we are dealing with and not the complex form (18), which has exhausted its utility in the preceding Section. It should be noted that adding a slow time dependence to the coefficients a b and c amounts to the Krylov-Bogoliubov technique which will be used in the subsequent Section.

To find the spectrum i.e. the set $\{\nu_k\}$ we go back to the equation of motion (19). The product nonlinearities ωi_{ra} and ωi_{rb} on the left hand side (LHS) of (19a,b) imply that if any ν_p and ν_q (and their negatives) belong to the spectrum then $\nu_p \pm \nu_q$ must also belong to it. Terms like $\omega \sin\Omega_1 t$ and $\omega \sin\Omega_2 t$ on the RHS imply that if any ν_p belongs to the spectrum then $\nu_p \pm \Omega_1$ and $\nu_p \pm \Omega_2$ also belong to the spectrum. Terms like $\Omega_1 \sin\Omega_1 t$ etc. on the RHS imply that $\nu = \pm\Omega_1, \pm\Omega_2$ belong to the spectrum. Finally, the term Γ on the RHS of (19c) is actually ν=0 so this too is a member of the spectrum. Clearly, the set satisfying all these conditions is

$$\{\nu_k\} = \{m\Omega_1 + n\Omega_2 ; m, n \in \mathbf{Z}\} \quad . \tag{24}$$

Note that this set is infinite and that its elements come arbitrarily close to any given number, hence the frequency spectrum is for all practical purposes continuous. This spectrum also appears in the study of the quasiperiodic Mathieu equation in the References. In the light of this observation we may modify our ansatz to write

$$i_{ra} = \int_{-\infty}^{\infty} a(\nu) \mathrm{e}^{\mathrm{j}\nu t} \, \mathrm{d}\nu \quad , \tag{25a}$$

$$i_{rb} = \int_{-\infty}^{\infty} b(\nu) \mathrm{e}^{\mathrm{j}\nu t} \, \mathrm{d}\nu \quad , \tag{25b}$$

$$\omega = \int_{-\infty}^{\infty} c(\nu) \mathrm{e}^{\mathrm{j}\nu t} \, \mathrm{d}\nu \quad . \tag{25c}$$

We must remember that i_{ra}, i_{rb} and ω are real so $a(\nu) = a^*(-\nu)$ and similarly for the other two variables. We then substitute this ansatz into (19) and attempt to balance the coefficient of $\mathrm{e}^{\mathrm{j}\nu t}\mathrm{d}\nu$ on LHS and RHS for any arbitrary value of ν. For (19a) this procedure yields

$$\begin{aligned} &\left(\mathrm{j}\nu + \frac{1}{\tau}\right) a(\nu) + \int_{-\infty}^{\infty} b(\nu') c(\nu - \nu') \mathrm{d}\nu' + \int_{-\infty}^{\infty} c(\nu') b(\nu - \nu') \mathrm{d}\nu' + \frac{i_1}{\mathrm{j}2}\left[c(\nu - \Omega_1) - c(\nu + \Omega_1)\right] \\ &+ \frac{i_2}{\mathrm{j}2}\left[c(\nu - \Omega_2) - c(\nu + \Omega_2)\right] = \frac{i_1 \Omega_1}{\mathrm{j}2}\left[\delta(\nu - \Omega_1) - \delta(\nu + \Omega_1)\right] + \frac{i_2 \Omega_2}{\mathrm{j}2}\left[\delta(\nu - \Omega_2) - \delta(\nu + \Omega_2)\right] \end{aligned} \quad . \tag{26a}$$

Note that the two integrals appearing on the LHS are nothing but convolutions of b and c i.e. $b(\nu) \circ c(\nu)$. The δ function terms appear on the RHS because they are the Fourier transforms of periodic functions. After understanding these features of (26a) we write the transforms of the other two equations

$$\begin{aligned} &\left(\mathrm{j}\nu + \frac{1}{\tau}\right) b(\nu) - 2a(\nu) \circ c(\nu) - \frac{i_1}{2}\left[c(\nu - \Omega_1) + c(\nu + \Omega_1)\right] - \frac{i_2}{2}\left[c(\nu - \Omega_2) + c(\nu + \Omega_2)\right] \\ &= \frac{i_1 \Omega_1}{2}\left[\delta(\nu - \Omega_1) + \delta(\nu + \Omega_1)\right] - \frac{i_2 \Omega_2}{2}\left[\delta(\nu - \Omega_2) + \delta(\nu + \Omega_2)\right] \end{aligned} \quad , \tag{26b}$$

$$\mathrm{j}\nu c(\nu) - \frac{C_0}{2J}\begin{bmatrix} -\mathrm{j}i_1\{a(\nu - \Omega_1) - a(\nu + \Omega_1)\} - \mathrm{j}i_2\{a(\nu - \Omega_2) - a(\nu + \Omega_2)\} \\ -i_1\{b(\nu - \Omega_1) + b(\nu + \Omega_1)\} - i_2\{b(\nu - \Omega_2) + b(\nu + \Omega_2)\} \end{bmatrix} = -\frac{\Gamma}{J}\delta(\nu) \quad . \tag{26c}$$

Equation (26) is of course the equation of motion in Fourier space.

These transform domain equations look formidable and we attempt a numerical solution instead of an analytical one. To do this, we first discretize the frequency space by considering a finite number of frequencies instead of the entire real line. Specifically, we take $-N \le m, n \le N$ in (26) for some integer N. Note that this yields a total of $N_1 = (2N+1)^2$ frequencies, no two of which can be equal. We sort these frequencies into an array $Nu[k]$ where k denotes the array index and runs from 1 to N_1. Next, we discretize a, b and c into three arrays $A[k]$, $B[k]$ and $C[k]$ with $A[k]$ denoting the value of $a(\nu)$ at frequency $\nu = Nu[k]$ and similarly for the other variables. In the discrete form, the convolution gets represented as

$$(f \circ g)[k] = \sum_{l=1}^{l-1} f[l]\, g[k-l] \quad . \tag{27}$$

To incorporate the terms like $c(v\text{-}\Omega_1)$ etc. in the discrete case, we define for each k four indices m_1, m_2, n_1 and n_2 such that

$$\begin{aligned} Nu[m_1] &= Nu[k] - \Omega_1 \\ Nu[m_2] &= Nu[k] + \Omega_1 \\ Nu[n_1] &= Nu[k] - \Omega_2 \\ Nu[n_2] &= Nu[k] + \Omega_2 \end{aligned} \quad . \tag{28}$$

If any of these indices happen to fall outside the range 1 to N_1 (which occurs when we consider frequencies near the boundary of the array Nu) then it remains undefined and any array element with the corresponding index is assigned the value zero. Finally, the delta functions go away in the discrete system. With the notation thus defined, the equations we solve numerically are

$$\left(\frac{1}{\tau} + \mathrm{j}Nu[k]\right) A[k] + 2\sum_{l=1}^{k-1} B[l]C[k-l] + \frac{i_1}{\mathrm{j}2}\left(C[m_1] - C[m_2]\right) + \frac{i_2}{\mathrm{j}2}\left(C[n_1] - C[n_2]\right)$$

$$= \begin{cases} \pm\dfrac{i_1\Omega_1}{\mathrm{j}2} & \text{if } Nu[k] = \pm\Omega_1 \\ \pm\dfrac{i_2\Omega_2}{\mathrm{j}2} & \text{if } Nu[k] = \pm\Omega_2 \\ \text{zero} \\ \text{otherwise} \end{cases} \quad , \tag{29a}$$

$$\left(\frac{1}{\tau} + \mathrm{j}Nu[k]\right) B[k] + 2\sum_{l=1}^{k-1} A[l]C[k-l] - \frac{i_1}{2}\left(C[m_1] + C[m_2]\right) - \frac{i_2}{2}\left(C[n_1] + C[n_2]\right)$$

$$= \begin{cases} -\dfrac{i_1\Omega_1}{2} & \text{if } Nu[k] = \pm\Omega_1 \\ -\dfrac{i_2\Omega_2}{2} & \text{if } Nu[k] = \pm\Omega_2 \\ \text{zero} \\ \text{otherwise} \end{cases} \quad , \tag{29b}$$

$$\mathrm{j}Nu[k]C[k] + \frac{C_0}{2}\begin{bmatrix} \mathrm{j}i_1\{-A[m_1] + A[m_2]\} + \mathrm{j}i_2\{-A[n_1] + A[n_2]\} \\ +i_1\{B[m_1] + B[m_2]\} + i_2\{B[n_1] + B[n_2]\} \end{bmatrix}$$

$$= \begin{cases} -\Gamma & \text{if } Nu[k] = 0 \\ \text{zero otherwise} \end{cases} \quad . \tag{29c}$$

The technique we use for solving these equations is the iterative Newton-Raphson method. We do not dwell on the procedural details except to mention that there are $3N_1$ quadratic equations in $3N_1$ variables (all $A[k]$'s, $B[k]$'s and $C[k]$'s) hence the system is solvable but has huge number of roots. Appropriate selection of initial conditions and imposition of the criterion mentioned after (25) take us to the solution which is physically plausible. We present the results in Figs. 3 to 8 where we have used N=3 (hence N_1=49). For definiteness we have chosen the parameter values τ=0.1, i_1=i_2=1, C_0=15, Γ=1, Ω_1=10 and Ω_2=14.1421356 [first few digits of sqrt(2)].

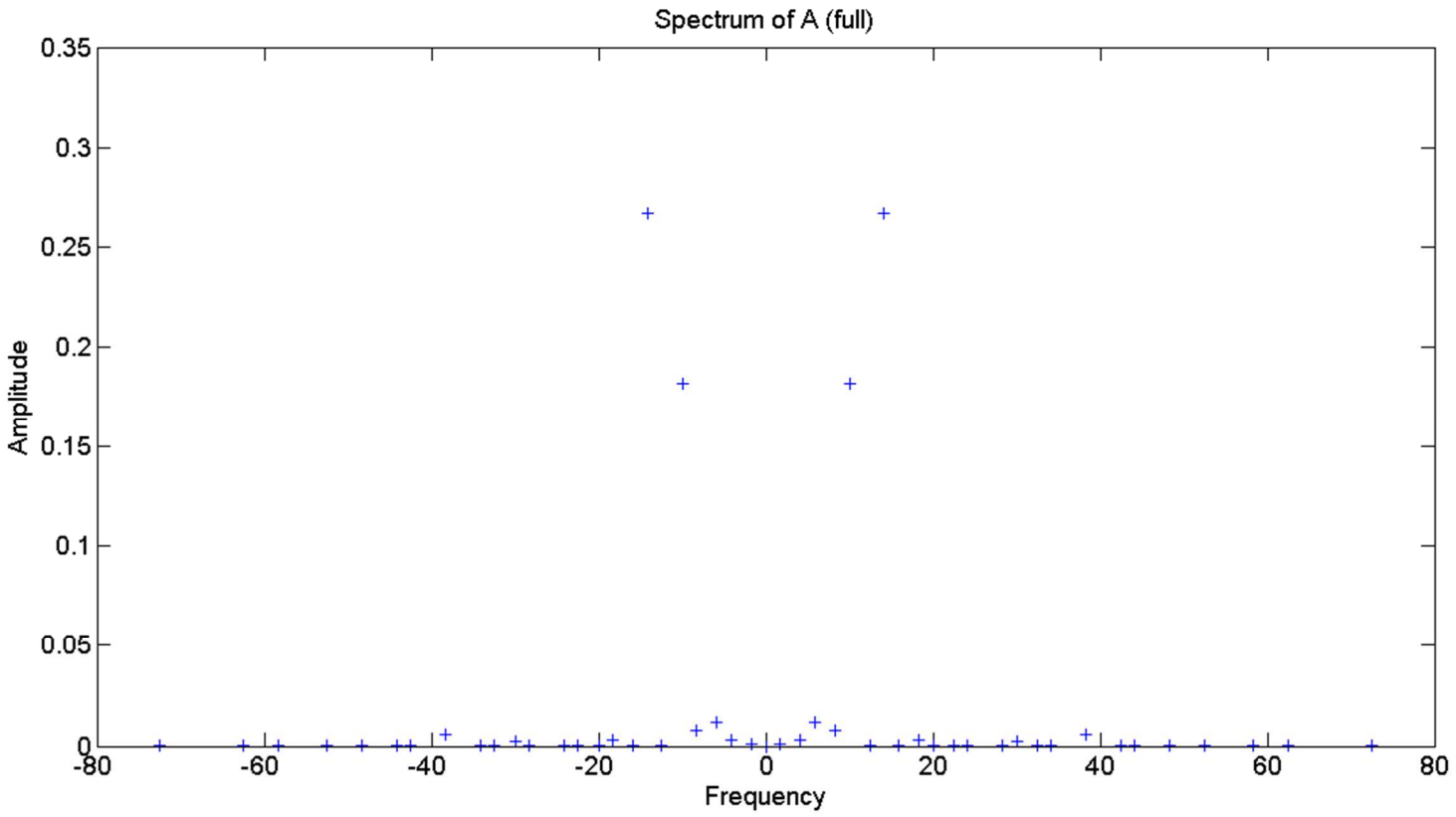

Figure 3 : *The spectrum of* a*(*ν*) in its discrete representation* A[k]*.* x*-axis shows* Nu*[*k*] while* y*-axis shows the modulus of* A[k]*for all* k *between 1 and* N*1. The figure is symmetric about* x*=0 on account of the condition that* a*(*ν*)=*a**(-*ν*). The spectrum peaks at the driving frequencies* Ω_1*=10 and* Ω_2*=14.1421356. Note that in the trivial case of one driving frequency, that is the only frequency where the response exists.*

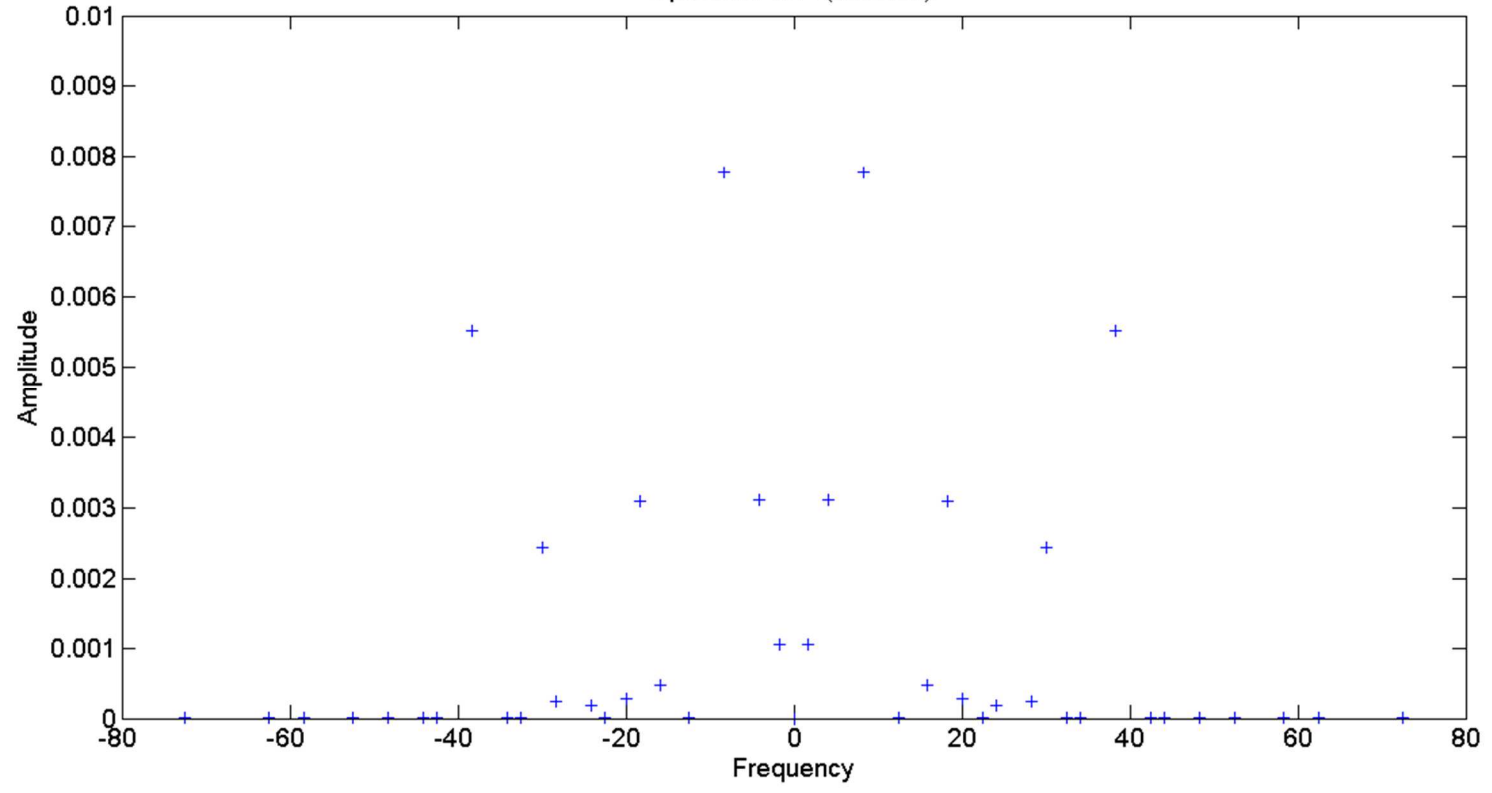

Figure 4 : *Zooming into the spectrum for* A *reveals the amplitudes at a host of frequencies other than the driving ones. The largest response occurs at (*m,n*)=(-2,2). The response at low frequency is also quite significant e.g. at the smallest frequency considered here, corresponding to (*m,n*)=(3,-2). Note the scale on the* y*-axis as against the previous figure.*

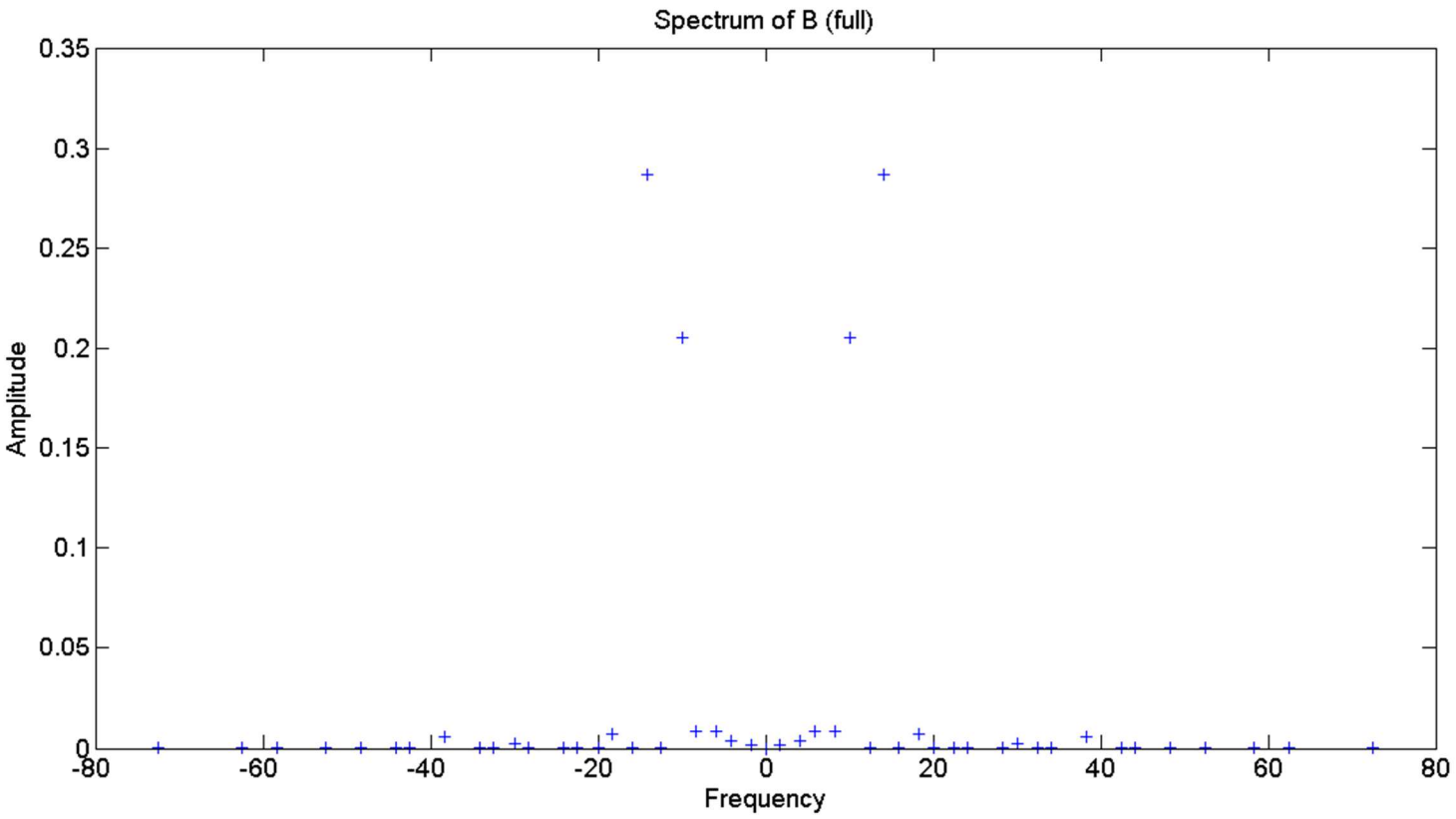

Figure 5 : *The full spectrum of* b(ν) *in the form* B[i]*. Comments same as for Fig. 2.*

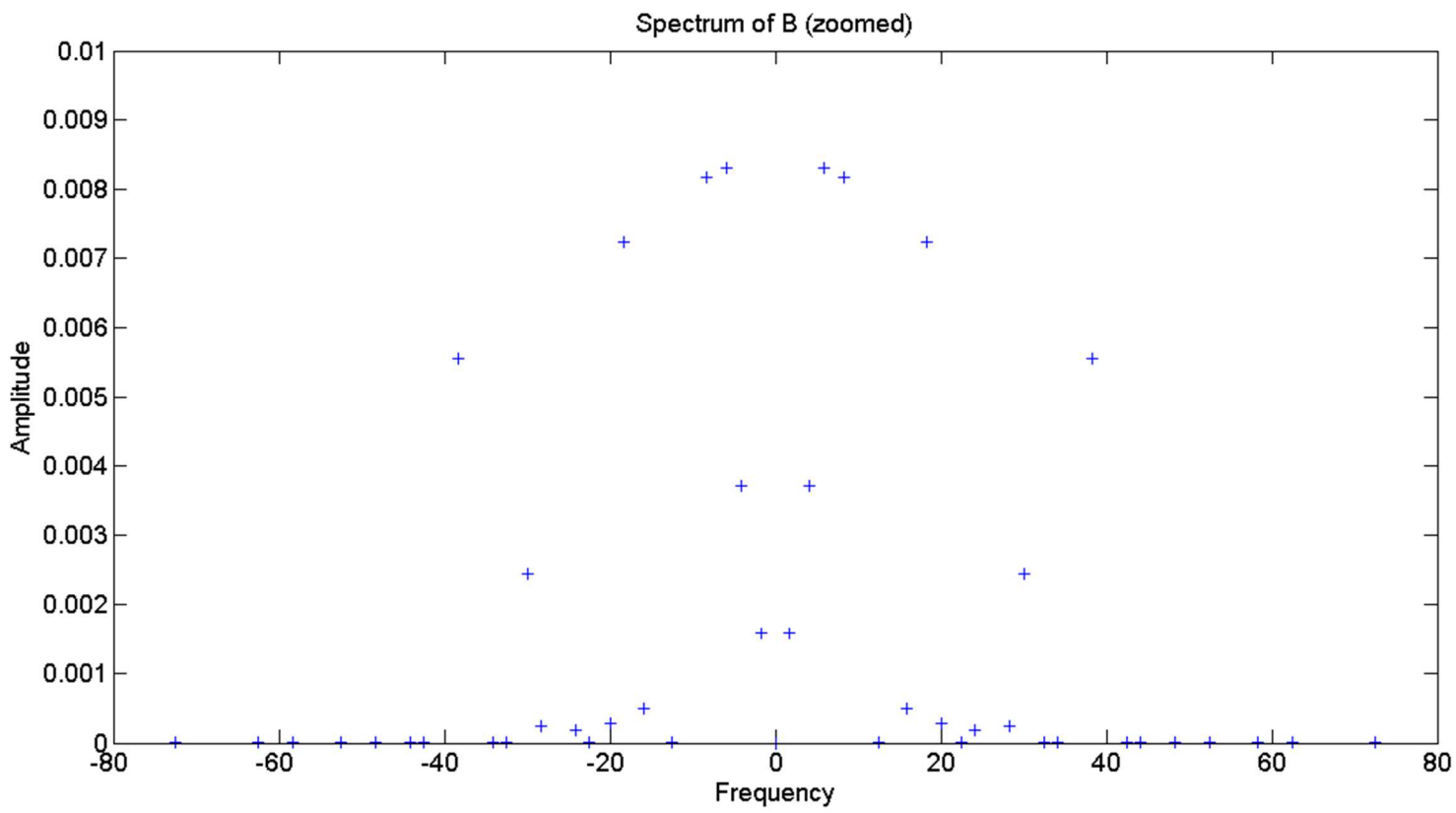

Figure 6 : *The zoomed-in spectrum of* b(ν)*. Comments same as for Fig. 3.*

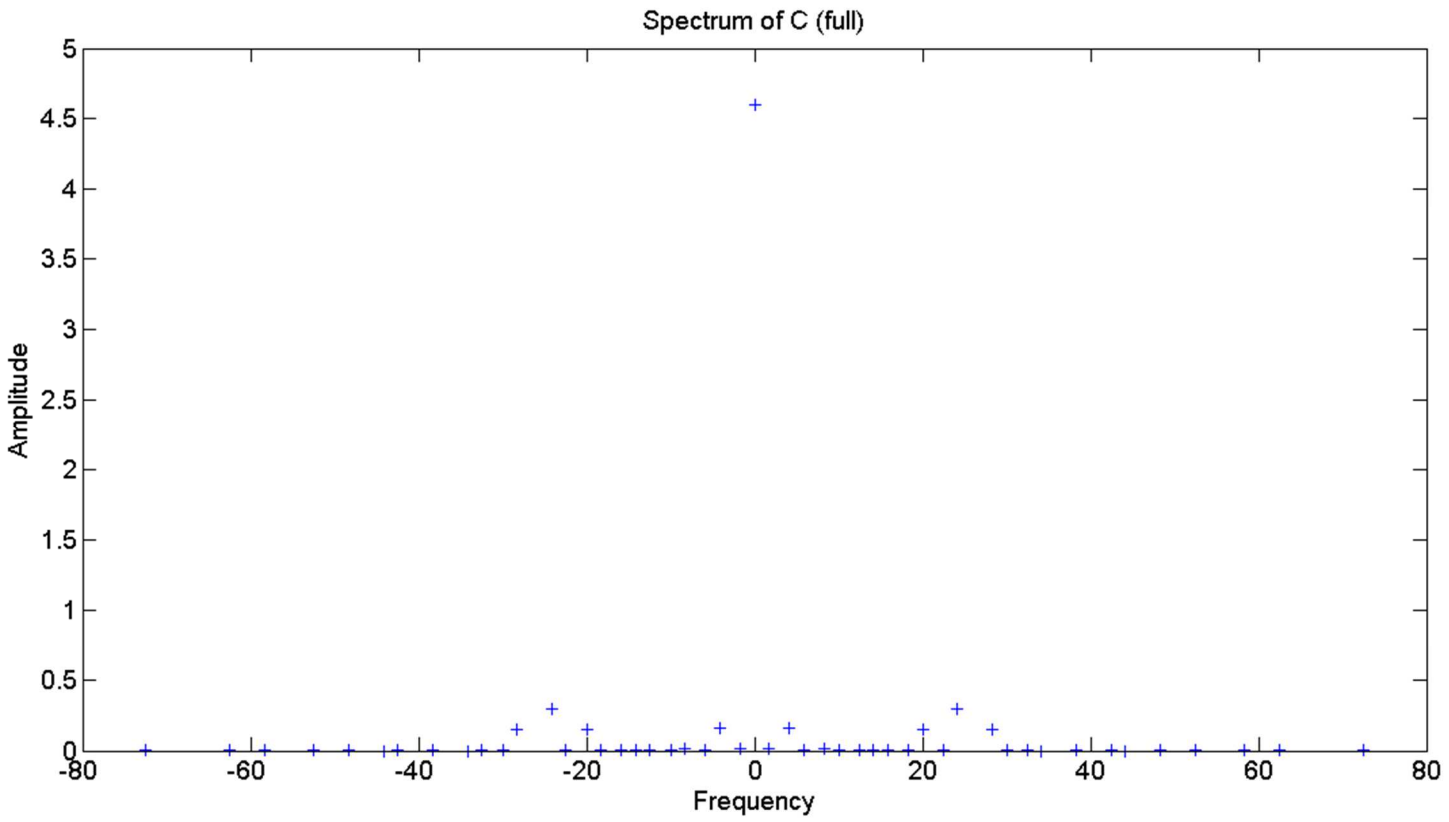

Figure 7 : *Full spectrum of* c(ν) *in the discrete representation. The peak is at* ν*=0. Note that in the trivial case of one driving frequency, 0 is the only frequency at which the response exists.*

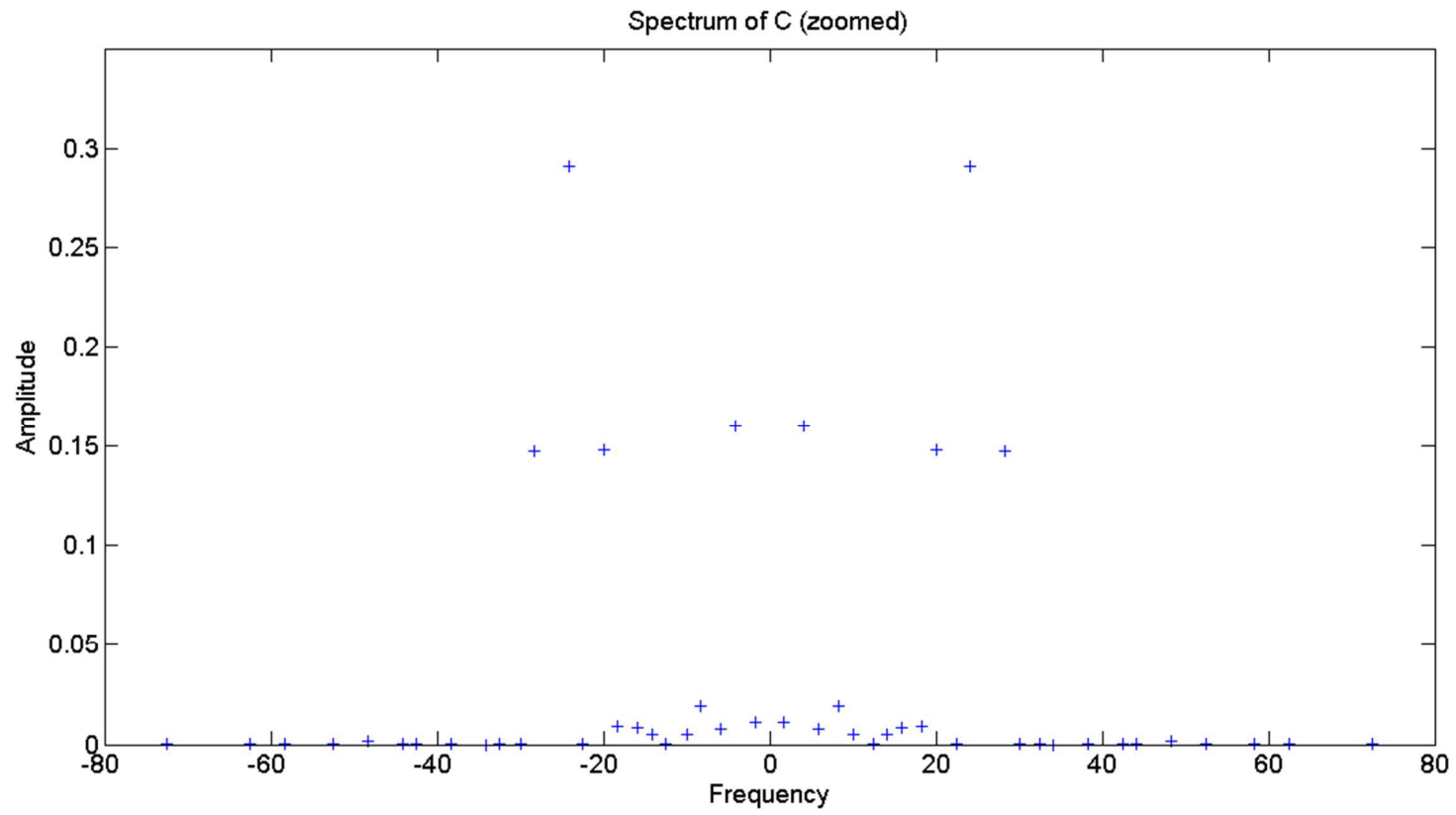

Figure 8 : *Zooming into the spectrum of* C*. Note that the driving frequencies* Ω_1 *and* Ω_2 *are not even minor players in this game.*

Our analytical predictions are confirmed through simulation (Figs. 9 and 10) where we numerically solve the equation of motion (19). In Fig. 9 the two main frequencies are readily apparent, through their sum and difference. Closer examination however reveals that the oscillations are not quite periodic with these frequencies and there are long-term differences in the shape of the trajectory. These long-term trends are even more prominent in Fig. 10 where the nature of oscillations fluctuates over tens of time units. The source of these trends is the response at ultra-low frequencies which we obtained in the analytical solution (Figs. 4, 6, 8). In these figures we can clearly see that there is a marked strength of response at low frequencies.

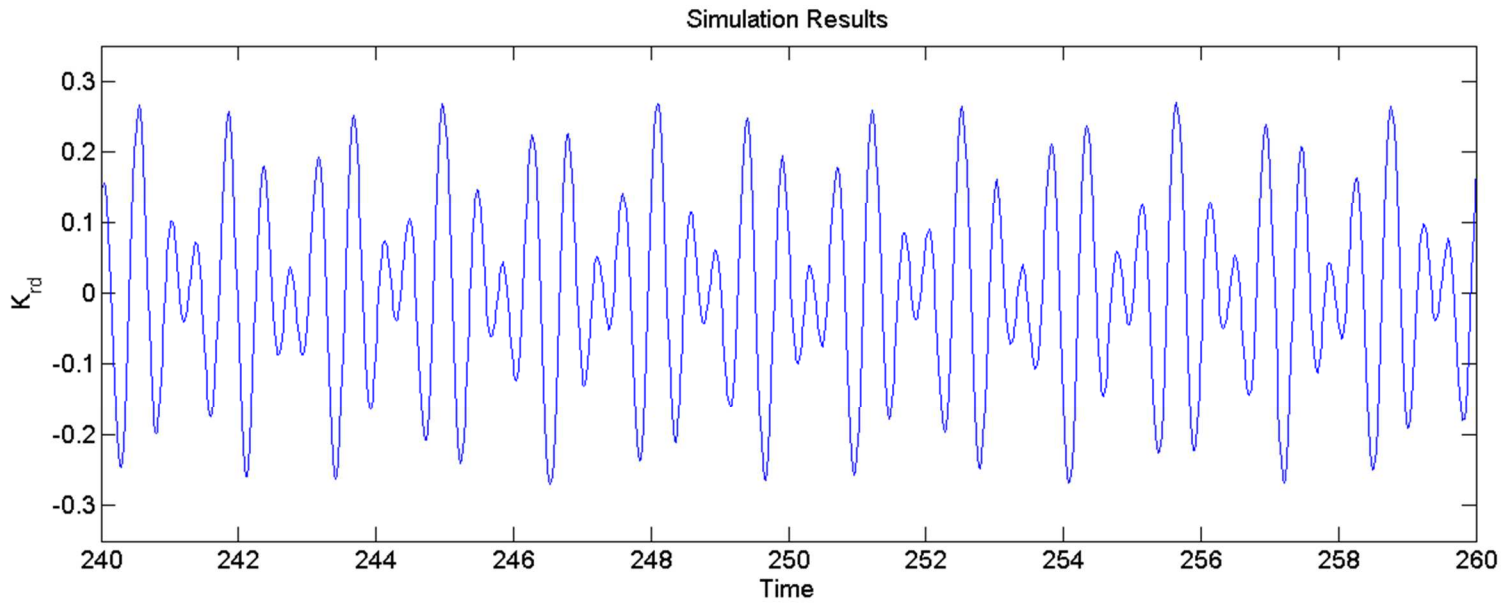

Figure 9 : *The actual run of the system is simulated. Two frequencies are readily apparent : the fast rate of appearance of successive local maxima (the average of the two driving frequencies) and the slower rate of appearance of approximately global maxima (the difference in the two driving frequencies). At a finer level, the pattern however is irregular – note the heights of the successive local maxima. Some features with long period are apparent – two successive local as well as near-global maxima occur at* t*=243 (a doublet), 247, 251 (a doublet), 255 etc. These suggest the presence of very low frequencies in the system.*

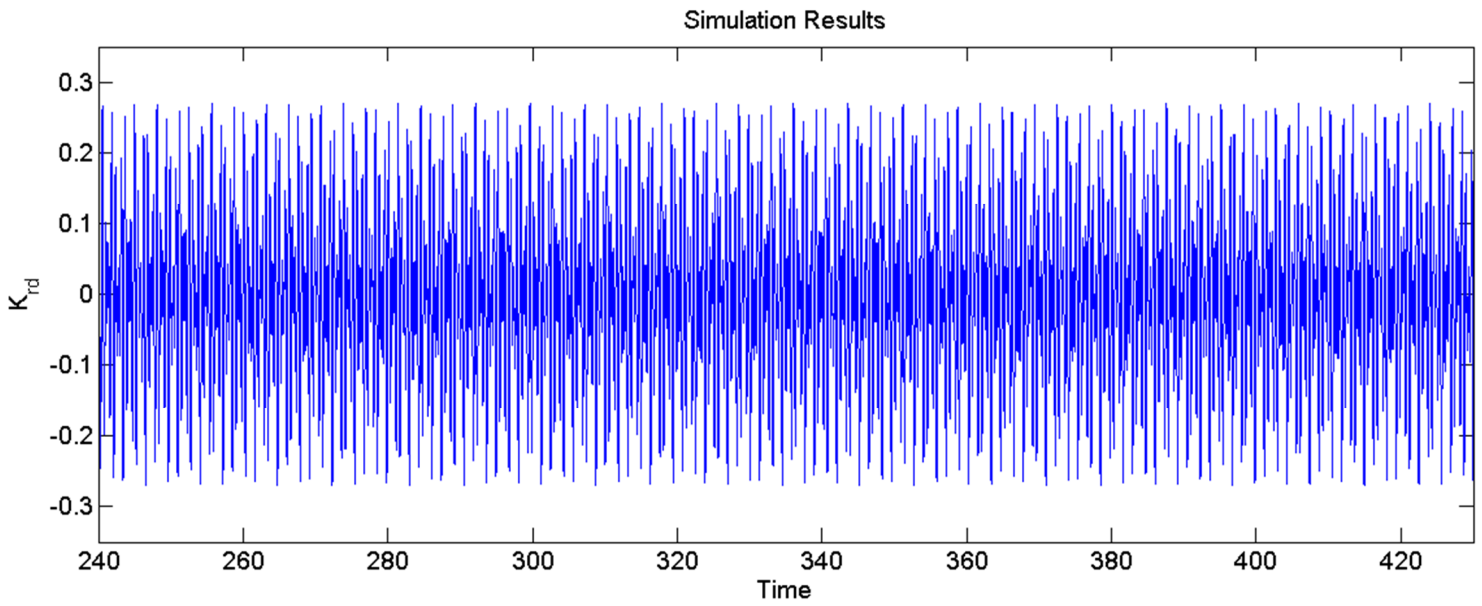

Figure 10 : *The simulation run for an extended period of time. Long-period behaviour in the shape of the central region of the oscillating plot is apparent.*

This completes the characterization of the quasiperiodic trajectories. It gives a detailed picture of the response frequencies which are having strong and weak amplitude. This analysis will come in useful in engineering problems like the one encountered by Belhaq op. cit. in which it is essential to know what will be the major vibration frequencies of the system under study. Having characterized the quasiperiodic trajectories we now turn to an analysis of their stability.

4. Stability of the quasiperiodic trajectory

We now start the Krylov-Bogoliubov stability analysis of the trajectories obtained in the above. A simplified case is one where the rotor moment of inertia J tends to infinity – in this case, ω becomes a constant and we get a solution similar to (20b) with two frequencies involved instead of one. This system is entirely equivalent to considering only the primary frequencies in the response spectra (Figs. 3,5,7) and neglecting all harmonics and combination frequencies. For this system, the Krylov-Bogoliubov machinery is quite straightforward and the result is the same as for the case of one driving frequency – the trajectory is stable for all parameter values. Simulations however show that this is quite far from reality when the moment of inertia is finite, especially if it is small. Above a certain value of C_0, the trajectory becomes unstable. To get this prediction analytically, we now perform the analysis on the full spectra obtained by us [15-17]. The starting point is of course the solution of the discrete Fourier-space system,

which we obtained in the previous Section. We let $A[k]$, $B[k]$ and $C[k]$ of (23), which we now denote using subscripts as A_k, B_k and C_k, be functions of time. We substitute ansatzes

$$i_{ra} = A_k(t)\mathrm{e}^{\mathrm{j}Nu_k t} + A_k{}^*(t)\mathrm{e}^{-\mathrm{j}Nu_k t} \quad , \tag{30a}$$

$$i_{rb} = B_k(t)\mathrm{e}^{\mathrm{j}Nu_k t} + B_k{}^*(t)\mathrm{e}^{-\mathrm{j}Nu_k t} \quad , \tag{30b}$$

$$\omega = C_k(t)\mathrm{e}^{\mathrm{j}Nu_k t} + C_k{}^*(t)\mathrm{e}^{-\mathrm{j}Nu_k t} \quad , \tag{30c}$$

into (19), noting that for the quasiperiodic trajectory itself, $A_k(t)$ etc. are all constant and equal to the values we found above. We make the assumption that near the trajectory, the time variation of any variable A_k, B_k and C_k is slow compared to expj($Nu_k t$) for any frequency Nu_k. Then, an expression like

$$\dot{A}_\alpha(t)\mathrm{e}^{\mathrm{j}Nu_\beta t} + B_\gamma(t)\mathrm{e}^{\mathrm{j}Nu_\beta t} = 0 \quad , \tag{31}$$

which arises from substituting (30) into (19), where α, β and γ are *arbitrary* values of k between 1 and N_1, can be simplified to

$$\dot{A}_\alpha(t) + B_\gamma(t) = 0 \quad . \tag{32}$$

With this assumption, we now repeat the steps leading to (26) i.e. balance the coefficient of expj($Nu_k t$) on LHS and RHS for all k. This leads to

$$\dot{A}_k(t) + \left(\frac{1}{\tau} + \mathrm{j}Nu_k\right)A_k(t) + 2\sum_{l=1}^{k-1} B_l(t)C_{k-l}(t) + \frac{i_1}{\mathrm{j}2}\left[C_{m1}(t) - C_{m2}(t)\right] + \frac{i_2}{\mathrm{j}2}\left[C_{n1}(t) - C_{n2}(t)\right]$$

$$= \begin{cases} \pm\dfrac{i_1\Omega_1}{\mathrm{j}2} & \text{if } Nu_k = \pm\Omega_1 \\ \pm\dfrac{i_2\Omega_2}{\mathrm{j}2} & \text{if } Nu_k = \pm\Omega_2 \\ \text{zero} \\ \text{otherwise} \end{cases} \quad , \tag{33a}$$

$$\dot{B}_k(t) + \left(\frac{1}{\tau} + \mathrm{j}Nu_k\right)B_k(t) - 2\sum_{l=1}^{k-1} A_l(t)C_{k-l}(t) - \frac{i_1}{2}\left[C_{m1}(t) + C_{m2}(t)\right] - \frac{i_2}{2}\left[C_{n1}(t) + C_{n2}(t)\right]$$

$$= \begin{cases} -\dfrac{i_1\Omega_1}{2} & \text{if } Nu_k = \pm\Omega_1 \\ -\dfrac{i_2\Omega_2}{2} & \text{if } Nu_k = \pm\Omega_2 \\ \text{zero} \\ \text{otherwise} \end{cases} \quad , \tag{33b}$$

$$\dot{C}_k(t) + \mathrm{j}Nu_k C_k(t) + \frac{C_0}{2}\begin{bmatrix} \mathrm{j}i_1\left\{-A_{m1}(t) + A_{m2}(t)\right\} + \mathrm{j}i_2\left\{-A_{n1}(t) + A_{n2}(t)\right\} \\ +i_1\left\{B_{m1}(t) + B_{m2}(t)\right\} + i_2\left\{B_{n1}(t) + B_{n2}(t)\right\} \end{bmatrix}$$

$$= \begin{cases} -\Gamma & \text{if } Nu_k = 0 \\ \text{zero otherwise} \end{cases} \quad . \tag{33c}$$

Note that this structure is the same as (29) except for the extra derivative terms and the time-varying nature of each variable. The trajectory itself is of course a fixed point of these dynamical equations. After the slowness, comes smallness – we now linearize by assuming that all the A_ks B_ks and C_ks are small perturbations from their trajectory values $A_k{}^f$ $B_k{}^f$and $C_k{}^f$which we found in Section 3. We let

$$A_k(t) = A_k^f + \Delta A_k(t) \quad , \tag{34a}$$

$$B_k(t) = B_k^f + \Delta B_k(t) \quad , \tag{34b}$$

$$C_k(t) = C_k^f + \Delta C_k(t) \quad . \tag{34c}$$

We substitute this into (33); by definition of fixed point the terms without Δ add up to zero and terms with 2 or more Δ's are dropped. This yields

$$\Delta\dot{A}_k = -\left(\frac{1}{\tau} + \mathrm{j}Nu_k\right)\Delta A_k - 2\sum_{l=1}^{k-1} B_l \Delta C_{k-l} - 2\sum_{l=1}^{k-1} C_l \Delta B_{k-l} + \frac{\mathrm{j}i_1}{2}\left(\Delta C_{m1} - \Delta C_{m2}\right) + \frac{\mathrm{j}i_2}{2}\left(\Delta C_{n1} - \Delta C_{n2}\right) , \tag{35a}$$

$$\Delta\dot{B}_k = -\left(\frac{1}{\tau} + \mathrm{j}Nu_k\right)\Delta B_k + 2\sum_{l=1}^{k-1} A_l \Delta C_{k-l} + 2\sum_{l=1}^{k-1} C_l \Delta A_{l-l} + \frac{i_1}{2}\left(\Delta C_{m1} + \Delta C_{m2}\right) + \frac{i_2}{2}\left(\Delta C_{n1} + \Delta C_{n2}\right) , \tag{35b}$$

$$\Delta\dot{C}_k = -\mathrm{j}Nu_k C_k - \frac{C_0}{2}\begin{bmatrix} \mathrm{j}i_1\left(-\Delta A_{m1} + \Delta A_{m2}\right) + \mathrm{j}i_2\left(-\Delta A_{n1} + \Delta A_{n2}\right) \\ +i_1\left(-\Delta B_{m1} + \Delta B_{m2}\right) + i_2\left(-\Delta B_{n1} + \Delta B_{n2}\right) \end{bmatrix} . \tag{35c}$$

We are almost done. The only step left before we can find the stability of the fixed point is the removal of j from the equations. This is done by separating out the real and imaginary parts of the ΔA_k s etc. – using a convenient engineering notation we write

$$\Delta A_k = \mathrm{Re}\left(\Delta A_k\right) + \mathrm{j}\,\mathrm{Im}\left(\Delta A_k\right) = \Delta A_i^d + \mathrm{j}\Delta A_i^q \quad \text{, similarly} \tag{36a}$$

$$\Delta B_k = \Delta B_k^d + \mathrm{j}\Delta B_k^q \quad , \tag{36b}$$

$$\Delta C_k = \Delta C_k^d + \mathrm{j}\Delta C_k^q \quad . \tag{36c}$$

We now use the simple identity

$$\begin{aligned} &\text{if } Z = XY \text{ then} \\ &Z^d = X^d Y^d - X^q Y^q \quad , \\ &Z^q = X^q Y^d + X^d Y^q \end{aligned} \tag{37}$$

to chase j away from (35). We get

$$\begin{aligned} \Delta\dot{A}_k^d = &-\frac{1}{\tau}\Delta A_k^d + Nu_k \Delta A_k^q - 2\sum_{l=1}^{k-1} B_l^d \Delta C_{k-l}^d + 2\sum_{l=1}^{ik-1} B_l^q \Delta C_{k-l}^q - 2\sum_{l=1}^{k-1} C_l^d \Delta B_{k-l}^d + 2\sum_{l=1}^{k-1} B_l^q \Delta C_{k-l}^q \\ &-\frac{i_1}{2}\left(\Delta C_{m1}^q - \Delta C_{m2}^q\right) - \frac{i_2}{2}\left(\Delta C_{n1}^q - \Delta C_{n2}^q\right) \end{aligned} \quad , \tag{38a}$$

$$\begin{aligned} \Delta\dot{A}_k^q = &-\frac{1}{\tau}\Delta A_k^q - Nu_k \Delta A_{kd} - 2\sum_{l=1}^{k-1} B_l^d \Delta C_{k-l}^q - 2\sum_{l=1}^{k-1} B_{k-l}^q \Delta C_{k-l}^d - 2\sum_{l=1}^{k-1} C_l^d \Delta B_{k-l}^q - 2\sum_{l=1}^{k-1} C_l^q \Delta B_{k-l}^d \\ &+\frac{i_1}{2}\left(\Delta C_{m1}^d - \Delta C_{m2}^d\right) + \frac{i_2}{2}\left(\Delta C_{n1}^d - \Delta C_{n2}^d\right) \end{aligned} \quad , \tag{38b}$$

$$\begin{aligned} \Delta\dot{B}_k^d = &-\frac{1}{\tau}\Delta B_k^d + Nu_k \Delta B_k^q + 2\sum_{l=1}^{k-1} A_l^d \Delta C_{k-l}^d - 2\sum_{l=1}^{k-1} A_l^q \Delta C_{k-l}^q + 2\sum_{l=1}^{k-1} C_l^d \Delta A_{k-l}^d - 2\sum_{l=1}^{k-1} C_l^q \Delta A_{k-l}^q \\ &+\frac{i_1}{2}\left(\Delta C_{m1}^d + \Delta C_{m2}^d\right) + \frac{i_2}{2}\left(\Delta C_{n1}^d + \Delta C_{n2}^d\right) \end{aligned} \quad , \tag{38c}$$

$$\begin{aligned} \Delta\dot{B}_k^q = &-\frac{1}{\tau}\Delta B_k^q - Nu_k \Delta B_k + 2\sum_{l=1}^{k-1} A_l^d \Delta C_{k-l}^q + 2\sum_{l=1}^{k-1} A_l^q \Delta C_{k-l}^d + 2\sum_{l=1}^{k-1} C_l^d \Delta A_{k-l}^q + 2\sum_{l=1}^{k-1} C_l^q \Delta A_{k-l}^d \\ &+\frac{i_1}{2}\left(\Delta C_{m1} + \Delta C_{m2}\right) + \frac{i_2}{2}\left(\Delta C_{n1} + \Delta C_{n2}\right) \end{aligned} \quad , \tag{38d}$$

$$\Delta\dot{C}_k^d = Nu_k \Delta C_k^q - \frac{C_0}{2}\left[i_1\left(\Delta A_{m1}^q - \Delta A_{m2}^q + \Delta B_{m1}^d + \Delta B_{m1}^d\right) + i_2\left(\Delta A_{n1}^q - \Delta A_{n2}^q + \Delta B_{n1}^d + \Delta B_{n2}^d\right)\right] \quad , \tag{38e}$$

$$\Delta\dot{C}_k^q = -Nu_k \Delta C_k^d - \frac{C_0}{2}\left[i_1\left(-\Delta A_{m1}^d + \Delta A_{m2}^d + \Delta B_{m1}^q + \Delta B_{m2}^q\right) + i_2\left(-\Delta A_{n1}^d + \Delta A_{n2}^d + \Delta B_{n1}^q + \Delta B_{n2}^q\right)\right] \quad . \tag{38f}$$

This equation finally describes the stability matrix and we must now find its eigenvalues numerically. Note that the size of this matrix is $6N_1$ squared; thus for the case N=3 [recall (24)] the matrix size is 294x294. The trajectory will be stable if all the eigenvalues have negative real parts; for the numbers taken in Section 3 we find that this is indeed the case (Fig. 11). The real parts are clustered in two primary regions, one close to $-1/\tau$ and the other close to zero, but all in the negative half-plane. Thus, the quasiperiodic trajectory is in fact stable; a prediction which is in agreement with simulation where the trajectories such as the ones shown in Figs. 9-10 are attained starting from virtually any initial condition.

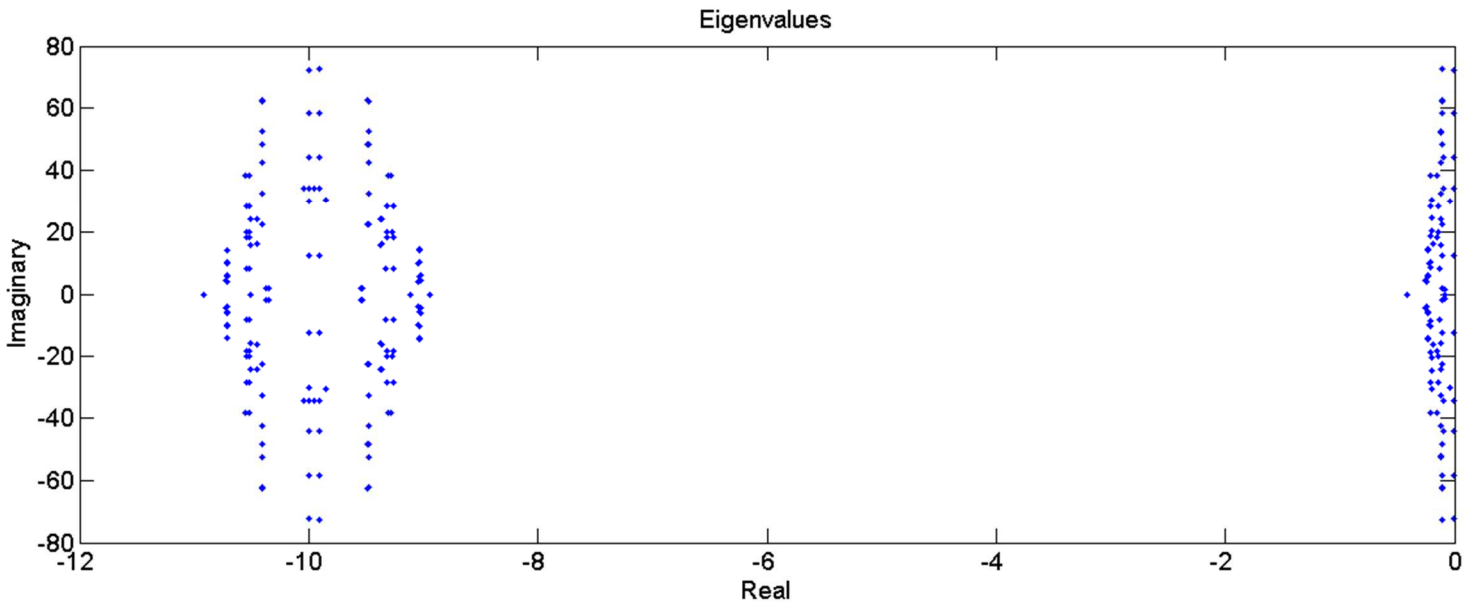

Figure 11 : *Eigenvalues of the Krylov-Bogoliubov stability matrix. Since τ has been taken as 0.1, the left hand set of eigenvalues are close to $1/\tau$. Note that all eigenvalues occur as complex conjugate pairs, which must be the case since the system under study is entirely real.*

The calculations also indicate that the stability can be affected by changing the parameter C_0. As C_0 increases, the eigenvalues split up into larger numbers of bands and then cross over into the positive real domain (Fig. 12-13). We make a brief comment regarding the manner in which we have observed this transition from negative real to positive real to take place. For values of C_0 close to zero, there are two bands of eigenvalues, one with real part just less than zero and the other with real part approximately $-1/\tau$. As C_0 increases, the ones near zero move leftward while the ones centred on $-1/\tau$ spread out wider and wider into more and more bands. Interestingly, it is these which eventually breach the zero line; at the critical value of C_0, exactly two of these acquire positive real parts while the imaginary parts remain finite. At this time, all other eigenvalues still retain their negative real parts.

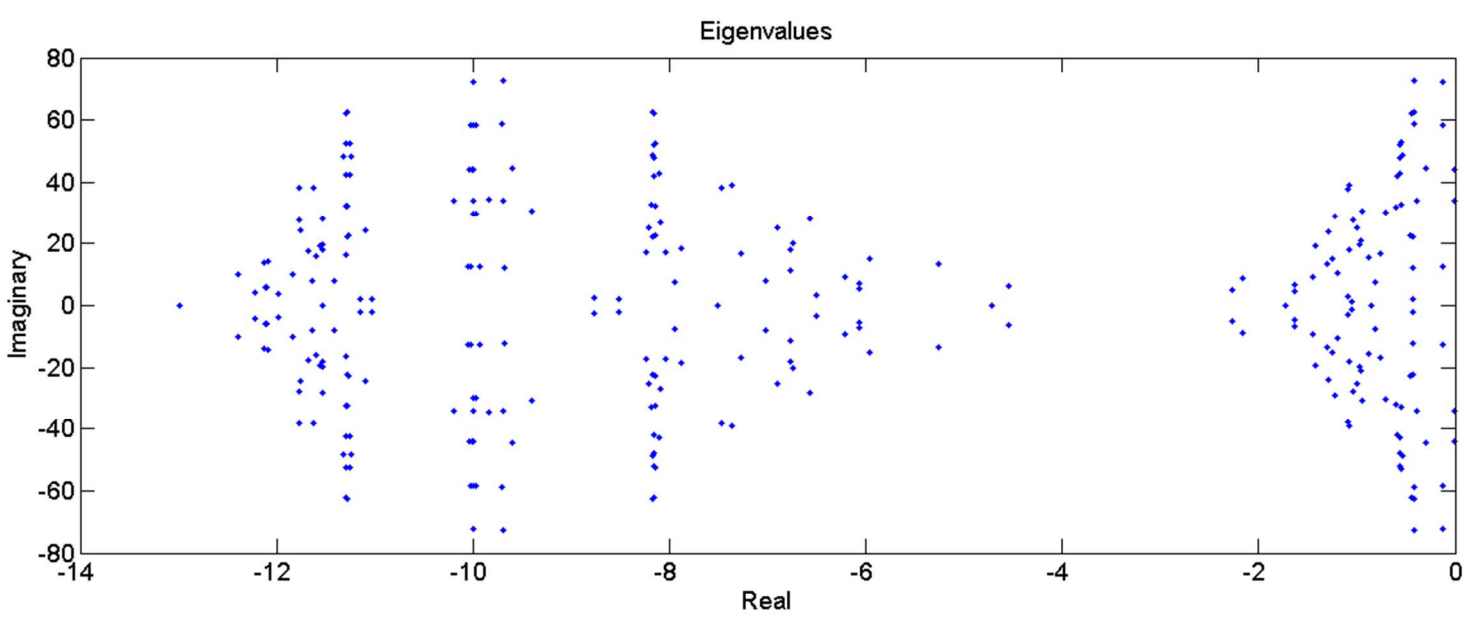

Figure 12 : *Plot of eigenvalues when C_0 is increased to 50. All the real parts are still negative.*

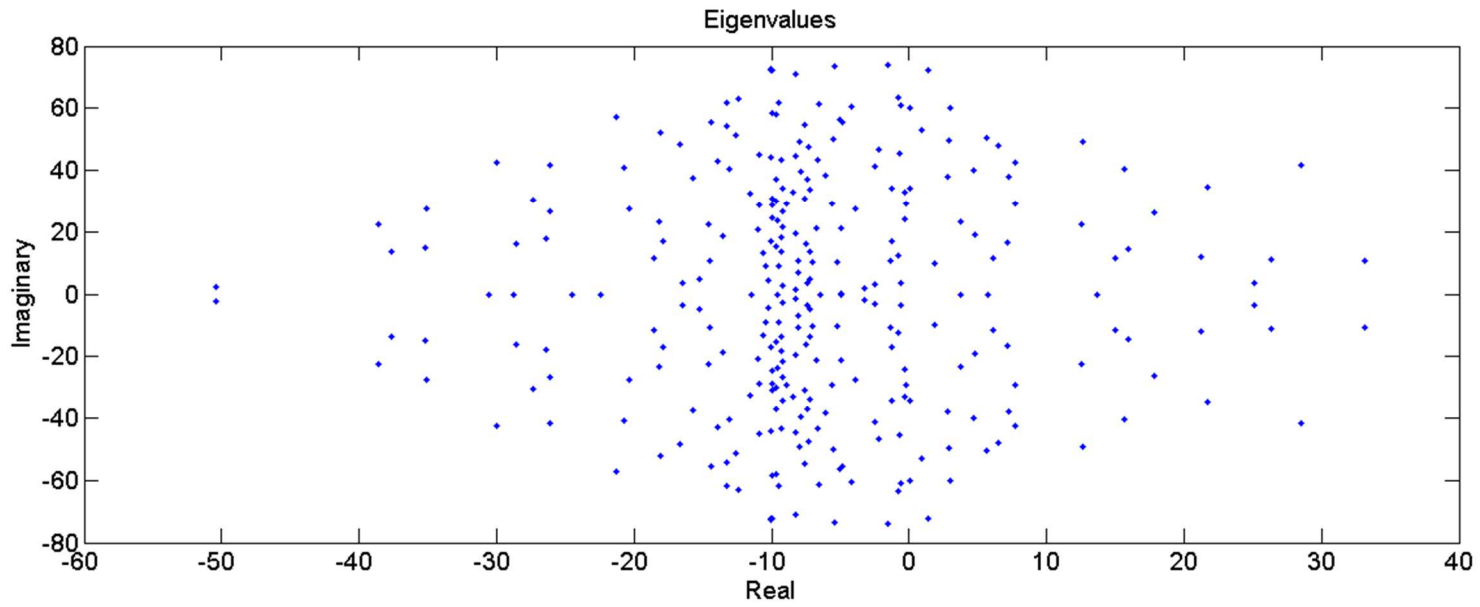

Figure 13 : *Plot of eigenvalues when C_0 is increased to 150. This time, many of the real parts are positive.*

The loss of stability as C_0 increases is physically intuitive : the larger the torque, the greater the oscillations in speed and the greater the oscillatory input in the current equations. Another way to make the system unstable is to make the currents strong while keeping C_0 unchanged. This too has the effect of magnifying the speed fluctuations and hence amplifying the oscillatory input to the current equations. In Fig. 14 we present a plot of the boundary of the stable region as the current (i_1 is assumed equal to i_2 and both have value i) and C_0 are varied. The curve shows a general decreasing trend, which is physically plausible – if the current is high then a weaker coupling constant C_0 will suffice to produce the required oscillations in speed. The plot also shows a few surprising jumps at some places. It would be interesting to find an explanation for the occurrence of these jumps.

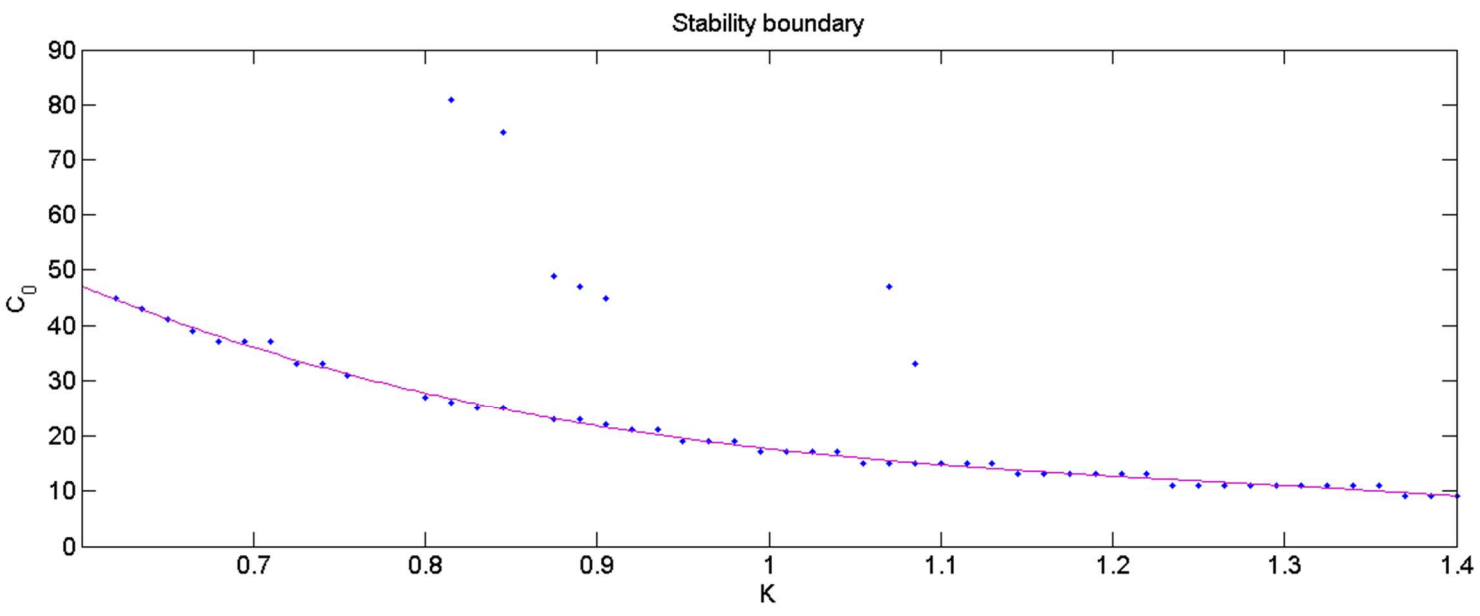

Figure 14 : *Stability boundary of the quasiperiodic state. The dots indicate data sets (i, C_0) above which the system becomes unstable. The purple line is obtained by fitting the bulk of the points; the decreasing trend is manifest. At a few locations however, the boundary points lie much above the average curve.*

Simulations confirm the existence of the boundary; they further show (Fig. 15) the trajectories becoming erratic and spinning off to infinity as time runs on.

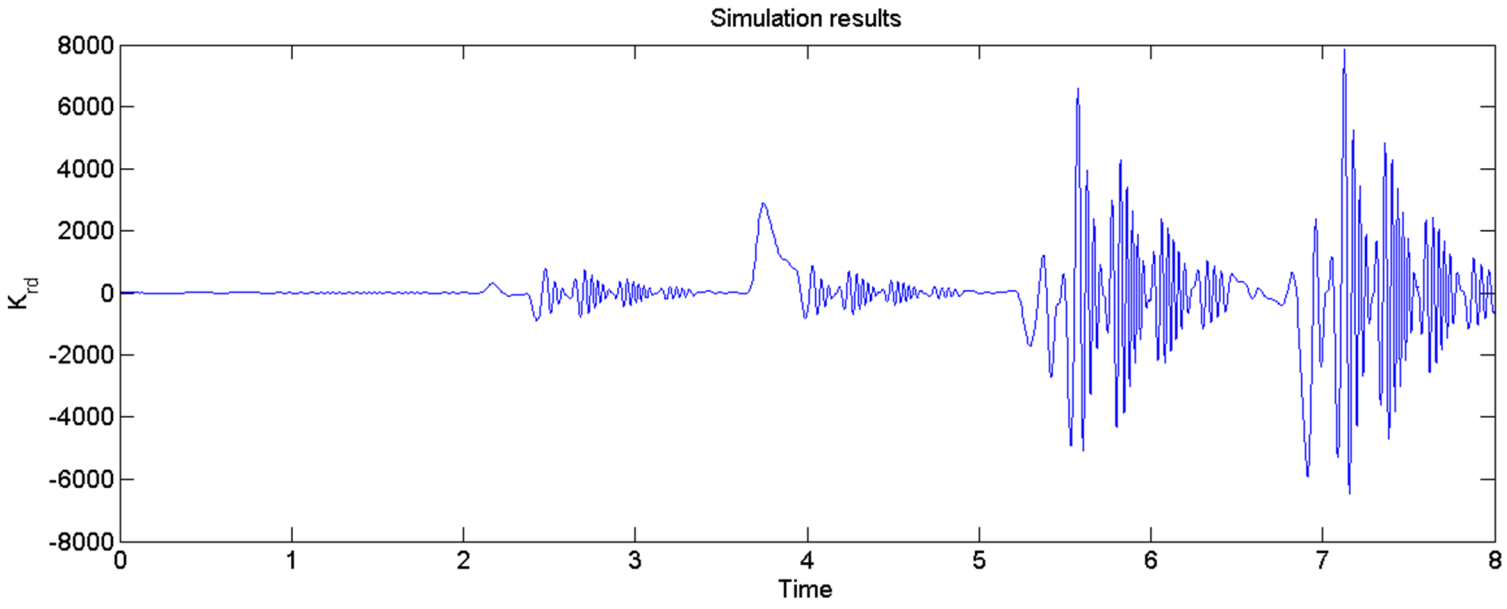

Figure 15 : *The system is simulated with C_0 taken as 5000. The diverging nature of the solution is clearly visible. If the run is continued, the amplitude increases more and more until it exceeds the computer's calculational capabilities.*

This divergence is of course unphysical. In reality, it will be curbed by three mechanisms : (a) rotor material not remaining magnetically linear but saturating, (b) rotor material not remaining electrically linear but acquiring extra impedance and (c) magnetostatic approximation, which is inherent in the derivation of (17) becoming invalid resulting in (19) ceasing to be the equation of motion. This indicates that the motion beyond the stability boundary will make for an interesting study in its own right – the system equations themselves will have to be re-derived before solution is attempted. The trajectories must of course remain bounded and we expect that they will show chaos as per the Ruelle-Takens prescription [18,19].

Before closing this Article we feel the need for one final comment. Suppose we tried analysing (19) perturbatively. Then we would start off by assuming the simplest form for ω, namely a constant. Under this assumption, (19a) and (19b) would reduce to the following equation for i_{rb} :

$$\frac{\mathrm{d}^2}{\mathrm{d}t^2}i_{rb}+\frac{2}{\tau}\frac{\mathrm{d}}{\mathrm{d}t}i_{rb}+\left(\frac{1}{\tau^2}+\omega^2\right)i_{rb}-i_1\left(\Omega_1^2-\omega^2\right)\sin\Omega_1 t-i_2\left(\Omega_2^2-\omega^2\right)\sin\Omega_2 t+$$
$$\frac{i_1}{\tau}\left(\Omega_1-\omega\right)\cos\Omega_1 t+\frac{i_2}{\tau}\left(\Omega_2-\omega\right)\cos\Omega_2 t=0 \qquad (39)$$

We now want to include a second order term in ω over and above the constant term. Equation (19c) indicates that such a term should have oscillations at $2\Omega_1$ and $2\Omega_2$. When this ω is substituted into (39), an equation like (13) will be formed, which has an intricate resonance structure. Nevertheless, when the full system (19) is simulated near such a resonance, we do not find any divergent behaviour. An example of this is shown in Fig. 16. The two driving frequencies are chosen as Ω_1=10 and Ω_2=5. Then, as per the partial analysis, ω should have oscillations at frequencies 20 and 10 superposed on a constant part. Since (39) actually features ω^2 in the parametric forcing, the double of these frequencies i.e. 40 and 20 should appear there. Now, we adjust parameters so that the constant part of ω becomes very nearly 10. Setting $1/\tau$ as very small, the oscillator natural frequency now becomes nearly half of one of the parametric frequencies, a region at which (13) had a big resonance (Fig. 2). Hence the partial analysis above would predict a divergence occurring here. But simulation of (19) shows nothing unusual.

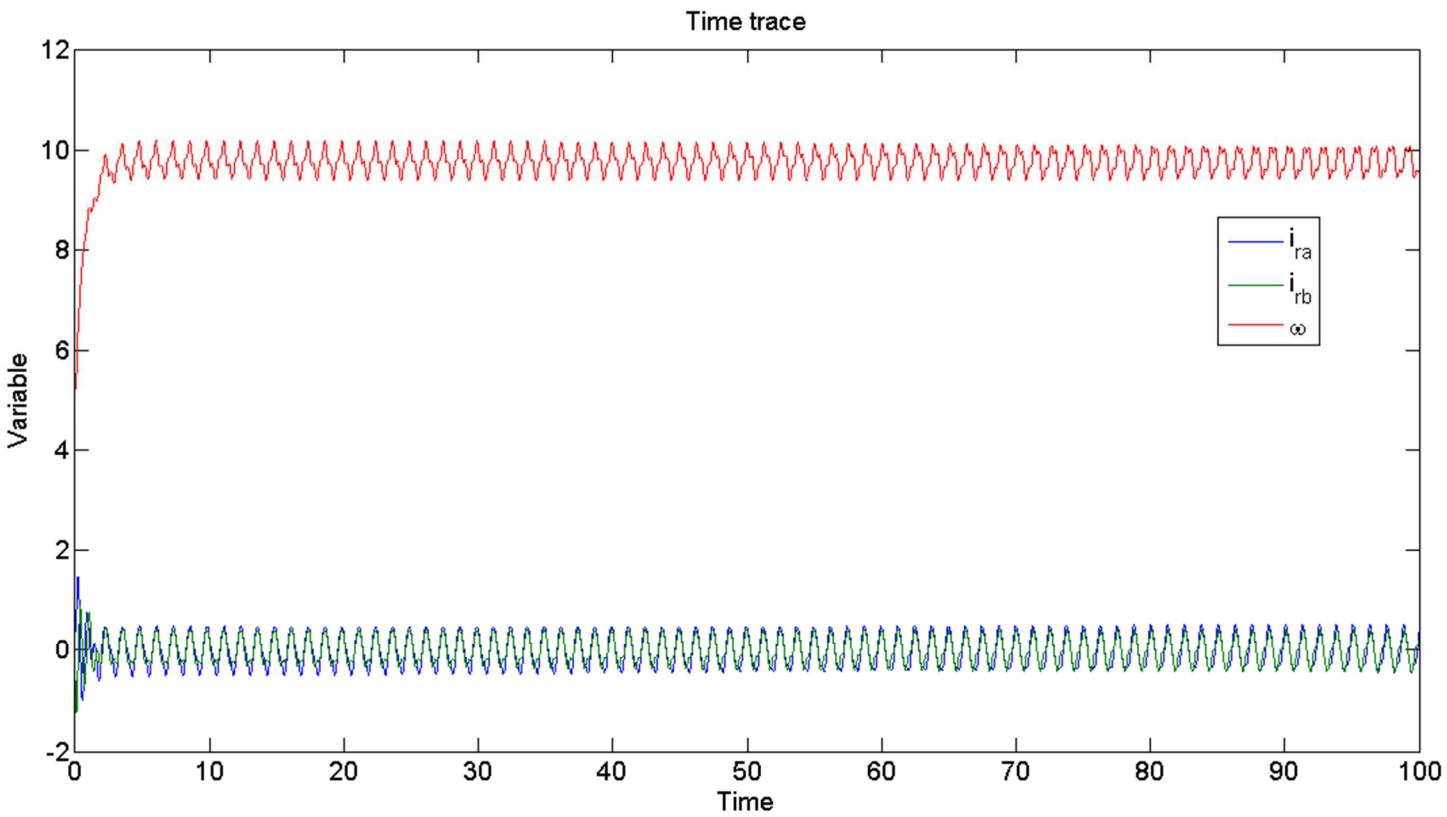

Figure 16 : *A plot of the motor variables for the case Ω_1=10 and Ω_2=5.01. Although the constant part of ω is indeed nearly 10, creating a potentially problematic situation, things remain under control.*

Thus we see that the effect of the full nonlinearity in (19) is to create stabilizing interactions which steer the system away from potential resonance zones.

We conclude the Article with a brief summary of the results obtained. We have proposed the Krylov-Bogoliubov technique as a common approach to solving Mathieu type equations with various forms of complications. Establishing the method by rederiving past results, we have then applied it to a situation where the quasiperiodic Mathieu equation also features quasiperiodic external excitation. A realistic system where such a situation arises is an induction motor so we have adopted that as our model. The Krylov-Bogoliubov analysis has yielded that the system is stable in typical operating regions. This stability is enhanced by the nonlinearities in the system which drive the dynamics away from potential resonance zones in the linearized forms.

* * * * *

Acknowledgement

We are grateful to Professor RICHARD RAND for helpful discussion and suggestions which have greatly improved the quality of this manuscript. Shayak is also grateful to Kishore Vaigyanik Protsahan Yojana (KVPY) Government of India for a generous Fellowship.

References

[1] D W Jordan and P Smith, "Nonlinear Ordinary Differential Equations," 4th Edition, Oxford University Press, Oxford, UK (2007)
[2] R H Rand, R S Zounes and R Hastings, "A Quasiperiodic Mathieu equation," *The Richard Rand 50th Anniversary Volume of Nonlinear Dynamics*, World Scientific, SIngapoore (1997)
[3] R S Zounes, "An Analysis of the nonlinear quasiperiodic Mathieu equation," Doctoral Dissertation, Cornell University (1997)
[4] R S Zounes and R H Rand, "Transition curves for the quasiperiodic Mathieu equation," **SIAM Journal of Applied Mathematics** 58 (4), 1094-1115 (1998)
[5] R H Rand, K Guennoun and M Belhaq, "2:2:1 Resonance in the quasiperiodic Mathieu equation," **Nonlinear Dynamics** 31, 367-374 (2003)
[6] N Abouhazim, R H Rand and M Belhaq, "The Damped nonlinear quasiperiodic Mathieu equation near 2:2:1 resonance," **Nonlinear Dynamics** 45, 237-247 (2006)

[7] T J Waters, “Stability of a 2-dimensional Mathieu-type system with quasiperiodic coefficients,” **Nonlinear Dynamics** 60, 341-356 (2010)
[8] G Kotowski, “Losungen der inhomogenen Mathieuschen Differential-gleichung mit periodischer storfunktion beliebiger frequenz (mit besonderer berucksichtigung der resonanzlosungen),” **Zeitschrift fur Angewande Mathematik und Mechanik** 23 (4), 213-229 (1943)
[9] M Belhaq and M Houssni, “Quasiperiodic oscillations, chaos and suppression of chaos in a nonlinear oscillator driven by parametric and external excitations,” **Nonlinear Dynamics** 18, 1-24 (1999)
[10] M Belhaq, I Kirrou and L Mokni, “Periodic and quasiperiodic galloping of a wind-excited tower under external excitation,” **Nonlinear Dynamics** 74, 849-867 (2013)
[11] R H Rand, “*Computer Algebra in Applied Mathematics : an Introduction to Macsyma*,” Pitman, Boston, Massachusetts, USA (1984)
[12] P K Kovacs and I Racz, “*Transient Behaviour in Electric Machinery*,” Verlag der Ungarische Akademie der Wissenschaften (1959)
[13] R Krishnan, “*Electric Motor Drives – Modeling, Analysis and Control*,” PHI Learning Private Limited, New Delhi (2010)
[14] D Cubero, J C Pascual and F Renzoni, “Irrationality and quiasiperiodicity in driven nonlinear systems,” **Physical Review Letters** 112, 174102 (2014)
[15] A H Nayfeh, “*Introduction to Perturbation Techniques*,” Wiley Interscience, New Jersey, USA (2011)
[16] L M Perko, “Higher order averaging and related methods for perturbed periodic and quasiperiodic systems,” **SIAM Journal of Applied Mathematics** 17 (4), 698-724 (1968)
[17] P Yu, Y M Desai, N Popplewell and A H Shah, “The Krylov Bogoliubov and Galerkin methods for nonlinear oscillations,” **Journal of Sound and Vibration** 192 (2), 413-438 (1996)
[18] D Ruelle and F Takens, “On the Nature of turbulence,” **Communications in Mathematical Physics** 20, 167-192 (1971)
[19] J Stavans, F Heslot and A Libchaber, “Fixed winding number and the quasiperiodic route to chaos in a convective fluid,” **Physical Review Letters** 55 (6), 596-599 (1985)